ASSESSMENT OF COLD WELDING BETWEEN SEPARABLE CONTACT SURFACES DUE TO IMPACT AND FRETTING UNDER VACUUM

A. MERSTALLINGER, M. SALES & E. SEMERAD
Austrian Institute of Technology

B.D. DUNN
ESA/ESTEC

European Space Agency

STM-279
November 2009

→ ASSESSMENT OF COLD WELDING BETWEEN SEPARABLE CONTACT SURFACES DUE TO IMPACT AND FRETTING UNDER VACUUM

A. MERSTALLINGER, M. SALES & E. SEMERAD
Austrian Institute of Technology (AIT),
A-2444 Seibersdorf, Austria

B.D. DUNN
Manufacturing Technology Advisor,
Product Assurance and Safety Department,
ESA/ESTEC, Noordwijk, the Netherlands

European Space Agency

An ESA Communications Production

Publication	*Assessment of Cold Welding between Separable Contact Surfaces due to Impact and Fretting under Vacuum* (ESA STM-279 November 2009)
Project Leader	K. Fletcher
Editing/Layout	Contactivity bv, Leiden, The Netherlands
Publisher	ESA Communication Production Office ESTEC, PO Box 299, 2200 AG Noordwijk, The Netherlands Tel: +31 71 565 3408 Fax: +31 71 565 5433 www.esa.int
ISBN	978-92-9221-900-6
ISSN	0379-4067
Copyright	© 2009 European Space Agency

Abstract

A common failure mode seen during the testing and operation of spacecraft is termed ‘cold welding’. European laboratories refer to this as ‘adhesion’, ‘sticking’ or ‘stiction’. This publication is intended to provide the space community with the most recent understanding of the phenomenon of ‘cold welding’ in relation to spacecraft mechanisms with separable contact surfaces. It presents some basic theory and describes a test method and the required equipment. Cold welding between two contacting surfaces can occur under conditions of impact or fretting. These surfaces may be bare metals, or inorganically or organically coated metals and their alloys. Standard procedures for quantifying the propensity of material surface pairs to cold weld to each other are proposed. Of particular interest will be the contact data of different materials, which are presented in numerical form and as tables summarising contacts between materials that can be either recommended or considered unsuitable for use under vacuum. The data have been compiled in a database that can be accessed online.

Keywords: Tribology, cold welding, space, fretting, coatings.

Contents

1 Introduction

1.1 Failures due to cold welding

Spacecraft subsystems contain a variety of engineering mechanisms that exhibit ball-to-flat surface contacts. These may be periodically closed up to several thousand times during ground testing and the operational life of the spacecraft. These contacts are usually designed to be static, but in reality they are often subjected to impact forces. Other static contacts are closed without impact, but will be subjected to fretting during the launch phase or during the deployment of arrays, as well as during the service life of the spacecraft. In the latter case, the fretting originates from vibrations of the spacecraft caused by gyros or the motion of antennas.

In most cases, metals are used in the construction of these mechanisms, preferably light metal alloys, but these are strongly prone to adhesion. Impacts and fretting also occur in terrestrial applications, but the main difference in space is the absence of atmospheric oxygen.

On the ground it is unusual to witness adhesion between metallic interfaces independently of whether they are subjected to impact or fretting. This is because the surfaces are re-oxidised after each opening, so that the next closing is made on new oxide layers. In space, the oxide layers are broken irreversibly. Therefore, the following closing is metal–metal contact, thereby enabling welding effects. In the literature, these effects may also be referred to as sticking, stiction or adhesion. Regarding ESA's space mechanisms, the relevant standard is ECSS-E-ST-33-01C [1], which uses the term 'separable contact surfaces'.

Impacts during closing can eventually degrade the mechanism's surface layers, whether they are natural oxides, chemical conversion films or even metallic coatings. This can dramatically increase the tendency of these contacting surfaces to 'cold weld' to each other. An example of such a mechanism is shown in Fig. 1. This picture illustrates how the Y-piece, manufactured from a magnesium alloy, has cold welded against one of the end-stops (labelled C in the figure), which is also made of a similar magnesium alloy. All corrosion protection coatings on these alloy parts have been worn away due to several hundreds of thousands of impacts to leave bare contacting points. The photograph shows the mechanism after ground-based tests performed under vacuum. Those test conditions replicated the conditions experienced by a similar mechanism that had failed in orbit on an Earth observation satellite. In technical terms, the adhesion forces were greater than the separation forces available from the spring in this mechanism. Ground simulation of the mechanism in a vacuum chamber indicated an adhesion force in the range of 0.3 N. This was later confirmed by impact testing at the Austrian Institute of Technology (AIT) [2].

Fig. 1. Example of a scanning mechanism from an Earth observation satellite. The Y-shaped so-called anchor is made to oscillate from its 'middle' resting position by electromagnetic forces. In doing so, the anchor continually impacts and is rebounded from each of the end stops. Eventually this anchor became cold welded to the end-stop, labelled C in the photograph.

Another, even more dangerous effect is **fretting.** Vibrations occurring during launch or during the movement of antennas in space, for example, can lead to small oscillating movements in the contact, which are referred to as 'fretting'. This lateral motion can cause even more severe surface destruction than impact,

and may lead to cold welding effects similar to bonding techniques. Adhesion forces may increase to values higher than the closing forces. One documented example of a failure due to cold welding after fretting occurred on the Galileo spacecraft in 1991 [3], when the high-gain antenna could not be fully deployed. The ribs of the umbrella-shaped antenna were locked for launch, but failed to open. Investigations have shown that fretting during transport and lift-off caused the ribs to cold weld together in the launch position.

1.2 Objective of the setup test method

'Cold welding' was first diagnosed as the cause of some spacecraft mechanism failures in the late 1980s and early 1990s. It was clear that laboratory testing was needed in order to assess the effects of different surfaces making 'static contact' under vacuum.

This was done by constructing two dedicated sets of equipment – an 'impact facility' and a 'fretting facility', both developed at AIT – which have been used to investigate several combinations of bulk materials and coatings for their tendency to 'cold welding'. The test philosophy is based on repeated closing and opening of a pin-to-disc contact. In an impact test, in each cycle, the contact is closed by an impact with a defined energy (no fretting applied). During a fretting test, the contact is closed softly (without impact), and while closed, fretting is applied to the contact. For both tests, the adhesion force, i.e. the force required to re-open the contact, is measured at each opening. Basic studies [4] were carried out to show the influence of the main parameters, the impact energy and the static load (contact pressure). These first results have been used to set up a standard test method with fixed parameters [5]. An overview of the test combinations is given in the following sections.

1.3 Background to the cold welding effect

Surfaces that are exposed to atmospheric conditions are generally covered by physically or chemically absorbed layers. Even in the absence of absorbed water, grease or other macroscopic contaminants, there remain surface layers, such as oxide and nitride layers, which are formed under terrestrial conditions on pure metal surfaces, and can be regarded as natural protection layers against cold welding.

Under vacuum or in a space environment, once these layers are removed by wear, they are not rebuilt and the exposed clean metal surfaces show a higher propensity to cold welding. So, their adhesive and tribological behaviours under vacuum or in a space environment differ significantly from those under terrestrial conditions, and the utility of data collected under the latter conditions is rather restricted. Second, the modelling of the adhesion forces suffers from the unknown degree of real metal–metal contact, which is linked to the destruction of the surface layers and is strongly affected by the contact situation. Moreover, most scientific studies are based on atomically clean surfaces. Hence, the adhesion values on typical surfaces of spacecraft produced by 'normal engineering' are somewhere between the high values seen from atomically clean surfaces and the 'too low values' derived from 'pure static' contacts. In a recent study, two theoretical approaches to calculate the adhesion forces were compared with experimentally measured adhesion forces for a fretting contact. It was shown that modelling approaches cannot predict the actual adhesion forces [6].

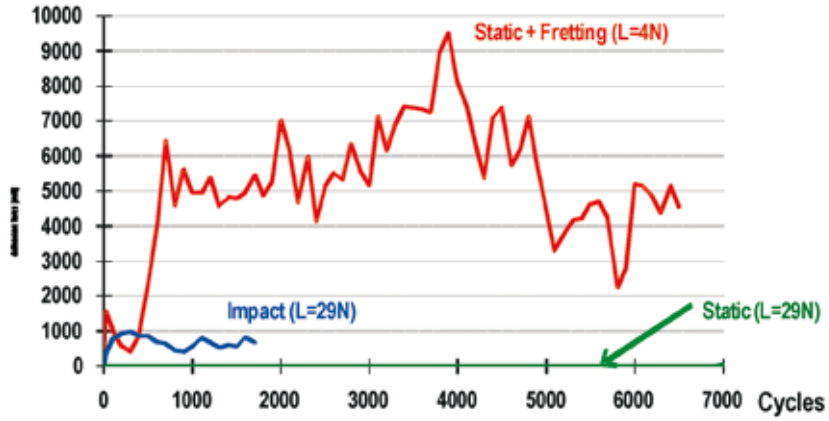

Fig. 2. Adhesion force as a function of the number of cycles (one closing and separation each) [8]. Comparison of adhesion under static (load 29 N), impact (load 29 N) and fretting (load 4 N) conditions under vacuum. The risk and severity of adhesion increase with contact in the order static, impact, fretting (maximum adhesion: static 0.1 N after >25 000 cycles; impact 0.96 N; and fretting 9.5 N).

From general experience [7], and as discussed in previous papers [8], [4], contact situations may be classified into three types: static, impact and fretting. In a cyclically closed and opened contact, the amount of destruction of the surface layers increases in the order: static, impact and fretting. As the surface layers are destroyed we see an increase in the adhesion forces. Figure 2 shows three plots of the adhesion force as a function of the number of cycles (= openings). The three plots refer to three types of contact applied to a pairing of titanium alloy (IMI834) and stainless steel (AISI 440C) [8]. Under fretting conditions, the maximum adhesion force throughout the test was 9.5 N (2.5 times the load of 4 N), under impact it was 0.96 N (load 29 N), whereas in static contact after 25 000 cycles the adhesion force was less than 0.1 N (load 29 N). A theoretical deduction would have given an estimate of 7.7 N without any relation to the real contact situation: the Hertzian contact area 0.006 mm^2 times the yield stress of this Ti alloy (~1200 MPa).

In summary, under impact and fretting conditions, contaminant layers (oxides) are removed much more quickly than under static contact, and cold welding occurs much sooner than expected. This may not only reduce the lifetime of a satellite, but can also endanger space missions, since any opening or ejection mechanism may fail due to cold-welded contacts. A typical opening/closing mechanism can fail if the adhesion force exceeds the force that is available to open the mechanism, e.g. by a spring. This ‘blocking’ value may be much lower than the applied load. The blocking of the mechanism shown in Fig. 1 under impact conditions was reported with an adhesion force in the range of 0.3 N. This value was confirmed by a verification study of the impact device [2].

2 Cold welding test method

The test method reported here is based on cyclic contacts. A pin is pressed onto a disc several thousand times. At each opening, the force required to separate the pin and the disc is measured, and is referred to as 'adhesion force' of this cycle. The adhesion force is plotted as a function of the number of cycles. The comparison of different materials is based on the maximum value of adhesion found for each material during a whole test.

To enable a comparison of the tendency of different material pairings to cold welding, the following test philosophy was set up at AIT (described in detail in an ARCS in-house specification [5]). The parameters static load and impact energy are fixed for each pairing with respect to the elastic limit (EL) of the contact pairing. Hertz's theory is used to calculate the contact pressure in the ball-to-flat contact. Using the yield strength of the softer material, the von Mises criterion defines an elastic limit: if the load (contact pressure) exceeds this EL, plastic yield will occur. Similarly, for the impact energy, a limit (W_Y) can be deduced, above which yielding occurs [5], [9].

Based on parameter studies [8], [4], an AIT standard was defined and approved by ESA: the static load is selected to achieve contact pressures of 40, 60 and 100% EL. An impact test begins with a static load, which achieves 40% EL. After 10 000 cycles, the load is increased to achieve 60% EL. After another 5000 cycles, loads of 100% EL are applied. The impact energy is kept constant at 40 times the limit W_Y. With this stepwise increase in load it is possible to obtain continuous data throughout a test run. (From the point of possible irreversible plastic deformation, the load may be increased but must not be reduced. In the latter case, work hardening of material might have increased hardness, so that the actual contact pressure is lower than calculated.)

For fretting tests, only one static load (related to 60% EL) is applied for 5000 cycles. The standard fretting test parameters are a stroke of 50 µm at a frequency of 200 Hz, as described fully in Annexes A and B. Uncoated specimens are freshly ground to a surface roughness of $R_a < 0.1$ µm before testing [5]. The contact is closed for 10 s and then and opened for another 10 s. At impact, the base pressure of the vacuum is less than 5×10^{-8} mbar, i.e. the surfaces are not recovered during opening. During a fretting test, a base pressure of 55×10^{-7} mbar is sufficient, since the change from oxidative to adhesive wear occurs in the range $0.1–10^{-3}$ mbar. The devices are described in Annex A, and a detail of the fretting test equipment is shown in Fig. 3.

The ECSS specification related to contact surfaces. ECSS ST E-33-01C, Part 3A, section 4.7.4.4.5, 'Separable contact surfaces' [1], states the following main requirements:

a) 'Peak Hertzian contact pressure shall be below 93% of the yield limit of the weakest material' (this refers to a contact pressure of 58% of the elastic limit, EL); and

d) '... the actuator shall be demonstrated to overcome two times the worst possible adhesion force ...'.

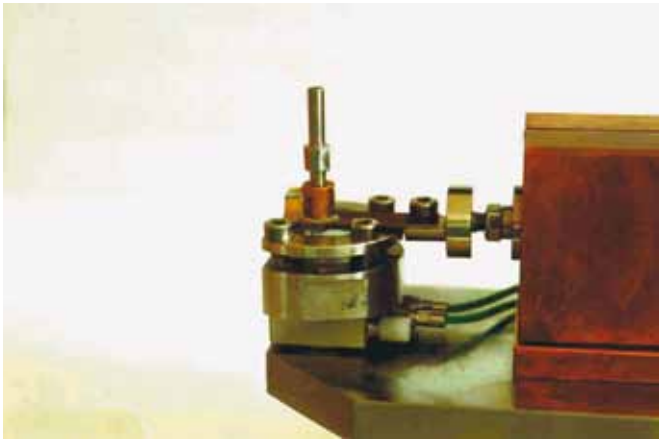

Fig. 3. Detail of the fretting device, showing the fixation of the pin (upper rod) and the disc (mounted directly on a force transducer). The piezo actuator that generates the fretting movement can be seen on the right.

Therefore, the results obtained from cold welding tests conducted in accordance with the ARC Seibersdorf (ARCS, now AIT) in-house specification [5] can be used to address the necessary opening forces for actuators in mechanisms (both impact and fretting tests are done at 60% EL).

A full description of the test equipment is given in Annex A. The test method [5] and the specimen geometries are given in Annex B. Several tests have been performed since the test method was standardised, and the results are compiled in Annex C (the data in Annex C can be obtained from the online database: *http://service.arcs.ac.at/coldwelddata*).

3 State of the art (ESA–AIT published data)

This section provides an overview of knowledge in the field of cold welding. It presents results related to the impact and fretting behaviours of materials and coatings, and describes some more general aspects such as the influence of contact parameters on adhesion.

3.1 Results of impact tests

3.1.1 Typical space materials under impact

In the following, data based on the worst case of impact (100% EL) are compared. Details of the materials and the abbreviations used are given in the tables in Annex C. A survey of adhesion forces observed for a selection of typical (uncoated) materials is shown in Fig. 4.

The highest adhesion is observed for stainless steel SS17-7PH in contact with itself (Fig. 4) or Al AA 7075 in contact with itself (1744 mN). This is an unexpected result, since titanium is usually regarded as the most ‘dangerous’ contact material. From a crystallographic point of view, face-centred cubic metals such as Fe and Al are most prone to adhesion due to their high ductility. A study of the adhesion of different working materials to a cutting tool made of high-speed steel [10] indicated a relation between the adhesion force and the Ni content. Regarding standard tests made with different steels in contact with themselves, the results show that the standard bearing steel (AISI 52100) has negligible adhesion. For the AISI 440C (no Ni) certain adhesion under impact was found. Mixing of steels can reduce adhesion (Fig. 5).

3.1.2 Influence of coatings on steel

Stainless steel discs (SS17-7PH) were coated with two types of coatings – hard (TiC) and soft (MoS_2) – and investigated for their ability to reduce adhesion.

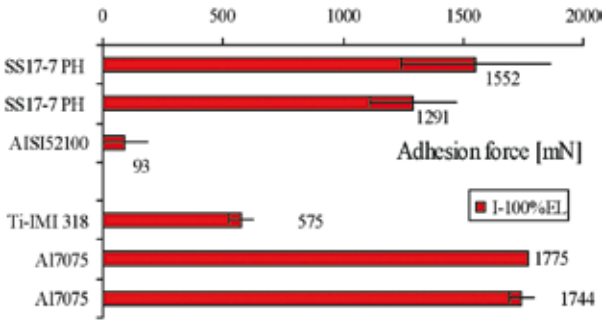

Fig. 4. Adhesion force under impact for materials in contact with themselves. The highest adhesion forces are found for stainless steels with nickel (e.g. SS17-7PH) and Al alloys (Al AA7075), medium for Ti alloy, and the lowest for bearing steel AISI 52100 (no Ni).

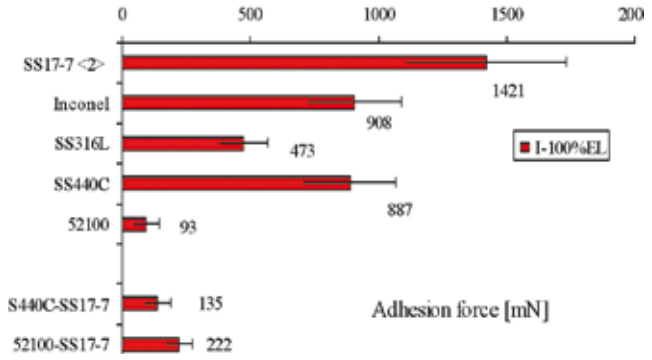

Fig. 5. Adhesion force under impact for different types of steel in contact with themselves: austenitic steels and Ni seem to promote high adhesion: SS17-7PH (7% Ni), AISI 316L (11% Ni) and Inconel 718 (52% Ni). No adhesion was found for AISI 52100 in contact with itself ('52100'). The high adhesion of AISI 440C has yet to be confirmed. With combinations of different steels, adhesion seems to increase in those in contact with steels with a higher tendency to cold welding (indicated by arrows).

The effectiveness of the first group of **hard coatings** depends on the load-bearing capacity of the underlying bulk: if it is too soft, it is deformed under impact, and the hard coating breaks [11]. Then the underlying metal comes into contact with the metal of the opposing surface, and adhesion occurs. However, pieces of the hard coating (TiC) are still present, and they may be transferred and act as additional abrasive particles. Hence, the adhesion may be reduced compared with bare metal surfaces, but since the destroyed surface areas cannot be 'recoated', adhesion still occurs. An example of this is **TiC** (2000 H_V) on SS17-7PH (only 441 H_V); the coating reduced the adhesion force by about four times, but after the TiC broke off it was no longer effective and a marked increase in the adhesion force was measured (see Fig. 6).

Hence, hard coatings should be applied to steel types that enable a higher hardness, e.g. AISI 440C or AISI 52100 (up to 700 H_V). This would avoid plastic deformation of the underlying steel substrate, which results in cracking of the coating.

Instead of using a hard coating, a harder steel type may be selected for contact with stainless steel SS17-7PH. By using steel AISI 52100 in contact with

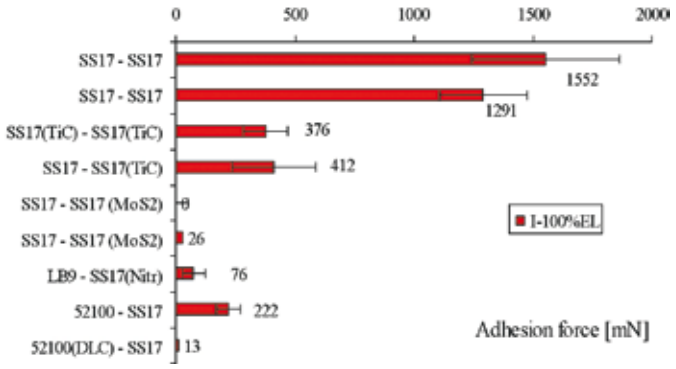

Fig. 6. Adhesion force as a function of static load for different coatings on steel. The lowest adhesion is for SS17-7PH (SS17) with MoS_2. The adhesion is highest for TiC (coatings were broken), and negligible between bronze (LB9) and SS17-7PH (LB9-SS17(Nitr)). The low adhesion between AISI 52100 and SS17-7PH can be further reduced by using a DLC coating ('52100(DLC)-SS17').

SS17-7PH, lower adhesion can be achieved (222 mN; see Fig. 5). This can be further reduced by applying a hard coating (diamond-like coating (DLC) produced by the company Vito) on hard steel [12] (Fig. 6). The hard **DLC film** did not (visibly) peel off and after more than 37 000 cycles no adhesion was measured. A small amount of steel was transferred from the (uncoated) pin to the DLC-coated disc. Before selecting DLC film, however, attention should be paid to its composition, since most conventional DLC coatings are not compatible with vacuum applications.

The second group of **soft coatings** was also tested. A **soft lubricant** coating on SS17-7PH could avoid any adhesion to another SS17-7PH pin. Hence, under impact, soft lubricant coatings on stainless steels are more effective than hard coatings in preventing cold welding.

3.1.3 Influence of coatings on aluminium and titanium

On the other hand, (hard) **finishes on soft aluminium** showed breaking and removal of the upper layers, but did not enable cold welding. Tests were run up to 50 000 cycles without finding sudden increases in adhesion forces. Figure 7 compares the maximum adhesion forces of Al AA7075 in contact with itself (uncoated: Al7075-Al7075) and the influence of selected coatings. No adhesion was found for the combinations Al AA7075 hard anodised versus stainless steel SS15-5PH ('Al7075(anod)-SS15') and Al AA7075 CrNi-coated versus Al AA7075 hard anodised ('Al7075(CrNi)–Al7075(anod)'). However, an Alodine 1200 coating only on the disc was not sufficient to prevent adhesion (Al7075(alod)-Al7075, adhesion force 336 mN).

A recently developed coating, named Keronite, also showed no adhesion, but the main advantage was that no surface destruction or formation of debris was found. Keronite is an advanced plasma electrolytic oxidation (PEO) treatment for the protection of light-weight metals such as those based on aluminium, magnesium and titanium [13] and [17].

Coatings on **Ti alloys** under impact can be divided into two groups: solid lubricants such as MoS_2 or Dicronite DL5 (WS_2) that do not prevent cold welding on Ti alloys, and hard coatings like Dicronite+, Balinite or Keronite that do (Fig. 8).

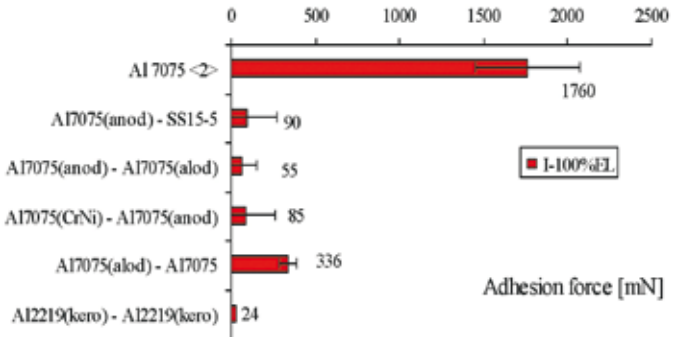

Fig. 7. Maximum adhesion force under impact for different coatings on aluminium (AA7075). The adhesion was negligible for combined coatings 'hard anodised (anod)', CrNi-plated (CrNi), Alodine 1200 (alod) and Keronite [13]. Alodine alone is not sufficient to prevent cold welding (336 mN) (for details of Keronite, see [13] and [17]).

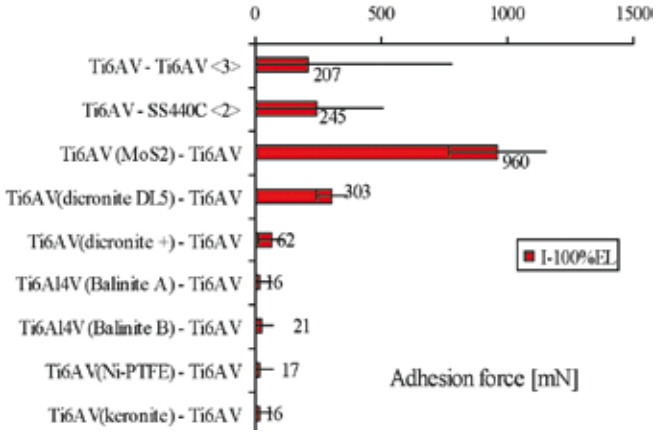

Fig. 8. Adhesion force under impact for different coatings on Ti alloys. Hard coatings provide good protection against cold welding, but solid lubricants (MoS_2, WS_2) fail.

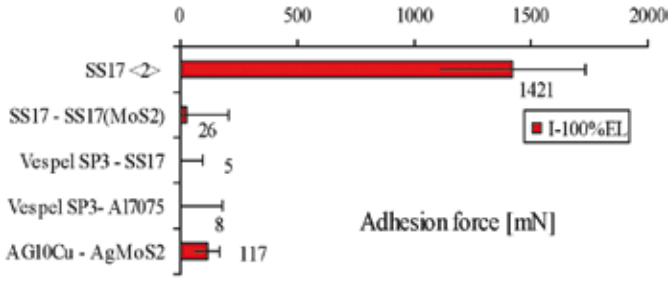

Fig. 9. Adhesion force under impact for different combinations with MoS_2. Coatings and composites are effective in preventing cold welding (SP3 = Vespel SP3, Ag10Cu = coin silver, $AgMoS_2$ = silver composite with 15 vol% MoS_2).

3.1.4 MoS_2 coatings versus MoS_2 composites

The investigations also included two composite materials containing MoS_2 particles: Vespel SP3 (polyimide with 15 mol% MoS_2) and a silver alloy, $AgMoS_2$ (with 15 vol% MoS_2). Vespel shows negligible adhesion against both stainless steels SS17-7PH and Al AA7075. The silver alloy shows low adhesion, 117 mN (the combination Ag10Cu versus $AgMoS_2$ is used in slip rings). SEM inspection showed the counter-surfaces to be (partially) covered with MoS_2 flakes that had been pressed out of the matrices. This effect is assisted by the fact that adhesion is mainly driven by bonding between two metals. In the case of Vespel SP3, no metal is present. In the case of silver, the very low shear strength enables easy breaking of the bonds. Hence, as well as coatings, composites also provide effective prevention of cold welding, due to their ability to reform; at each impact a new lubrication layer is formed and the uncoated areas are recoated (Fig. 9).

3.2 Results of fretting tests

3.2.1 Comparison of impact and fretting contacts

A survey of adhesion forces found under fretting and impact conditions is given in Fig. 10 (data from [12], [14], [15], [8], [16].) As mentioned in the introduction, fretting, which involves small sliding movements, was expected to cause severe surface destruction. In the highest allowed contact pressure at impact (100% EL), typical adhesion forces range up to approximately 2000 mN. Under fretting conditions at even lower contact pressures (60% EL), the adhesion forces exceed these values by up to a factor of 10. Stainless steel SS17-7PH in contact with itself shows adhesion of approximately 1500 mN under impact, but more than 11 000 mN under fretting (Fig. 10, 'SS17-7'). For other metal–metal contacts – Al AA7075 in contact with itself – similar behaviour is found [15]. The strongest adhesion is found for Inconel 718 (Ni alloy). No adhesion is found for polymer–metal contacts, such as Vespel SP3 (polyimide with 15 mol% MoS_2) versus stainless steel SS17-7PH.

As mentioned above, the adhesion of different construction steels to a cutting tool of high-speed steel indicated a relation between the adhesion force and Ni content under fretting conditions [10]. Standard fretting tests [5] done on different steels in contact with themselves also showed this basic relationship (Fig. 10). The adhesion decreases in the order Inconel 718 (52%Ni), SS17-7PH (7%Ni) and AISI 316L (11%Ni), down to AISI 52100 and even lower for AISI 440C (no Ni). The bearing steels (AISI 52100 and SS440C) show the lowest adhesion under fretting (the high adhesion of AISI 440C (no Ni) under impact is still under investigation).

3.3 Influence of coatings under fretting

3.3.1 Coatings on steel

The previous section has shown that certain alloys exhibit high adhesion. Therefore, typical coatings were investigated for their ability to prevent cold welding under fretting conditions. Figure 11 shows the results for **coatings**

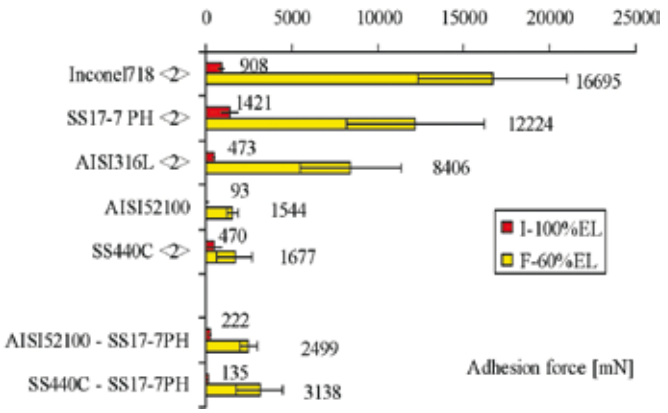

Fig. 10. Comparison of adhesion force under impact (I) and fretting (F) for different steels and Ni alloys in contact with themselves. Fretting initiates higher adhesion, but for ferrous alloys adhesion decreases with decreasing Ni content, as indicated in [10].

on steel compared with those for contacts between bare materials. Applying an **MoS_2 coating by PVD** to one of the two SS17-7PH counterparts could not prevent adhesion: in two tests the lubrication effect was lost after only 50 (20) cycles, i.e. 8 (3) minutes fretting or 100 000 (42 000) strokes. This was combined with a distinct increase in adhesion force. High adhesion forces of up to 5870 mN were found. This refers to a reduction in the maximum adhesion force of approximately 50% (compared with SS17-7 without coating) (Fig. 11). The same tendency can be seen for one **TiC coating** between two SS17-7PH counterparts (Fig. 11, 'SS17-SS17(TiC)'). Adhesion is only reduced to approximately one-third of that of the uncoated combination. SEM images and EDAX analyses confirm the breaking up of the coating and adhesive wear.

The influence of **nitriding** SS17-7PH surfaces was investigated, and no significant reduction in adhesion was visible (still 8517 mN; Fig. 11, 'SS17-SS17(nitr)'). Based on this result, the low adhesion between nitrided SS17-7 and lead-bearing bronze LB9 (500–1087 mN) may be due to the lubrication effect of the lead (which is known for its tribological applications).

Applying a **diamond-like coating (DLC)** onto AISI 52100 in contact with SS17-7PH reduces adhesion from 2499 mN to 856 mN.

The effect of **grease** (Braycote 601) was tested in AISI 440C in contact with itself, but no significant effect was observed. Hence the risk of contamination due to outgassing is superior to the efficiency in avoiding adhesion (Fig. 11, '440C(bray)-440C').

MoS_2 coating in a special pairing (AISI 440C+MoS_2 versus SS17-7PH+TiC): MoS_2 + TiC resulted in a breakthrough (at 366 cycles = 61 min = 700 000 strokes) and medium adhesion forces of up to 2210 mN. Applying only MoS_2 on a AISI 440C disc and testing it in contact with SS17-7PH, only very low

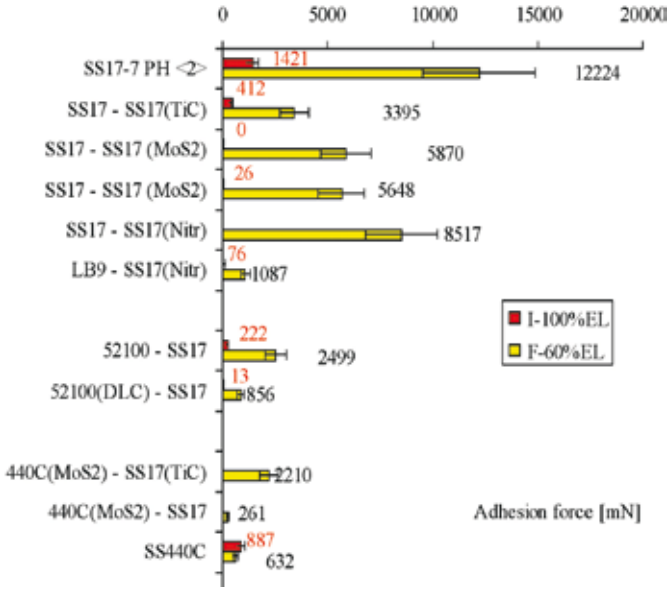

Fig. 11. Adhesion force of steel-based coatings under impact (I) and fretting (F) conditions. Coatings in general reduce adhesion. For SS17-7PH, no tested coating of the disc is able to reduce adhesion significantly (TiC, MoS_2 or nitriding). In contacts between AISI 440C and SS17-7PH, TiC should be avoided. The efficiency of grease (Braycote 601) is not significant in AISI 440C in contact with itself, and that of the MoS_2 coating under fretting is limited to low endurance

adhesion forces were found (compare with AISI 440C in contact with itself without coating; Fig. 11, 'SS440C'). It can therefore be concluded that the TiC destroys the surface layers of the AISI 440C, which could have been regarded as adhesion prevention layers.

3.3.2 Coatings on aluminium and titanium

Selected combinations of coatings on **aluminium** were tested under fretting conditions. No adhesion was found between Al AA7075 hard anodised and Al AA7075 NiCr-plated (see Fig. 12). Al AA7075 hard anodised in contact with uncoated SS15-5PH showed negligible adhesion. This is in contrast with the fact that SEM images show breakthrough and peeling off of the conversion layer on the Al. But the results are in accordance with those of impact tests [14]; despite a breakthrough of the layer, no adhesion was measured. Coating only the disc with Alodine did not prevent cold welding, and a medium adhesion of 2036 mN was found (Fig. 12, 'Al7075(alod)-Al7075'). Alodine 1200 is a chemical conversion coating composed of hydrated aluminium chromate, which is very thin (<1 µm). Therefore, the fretting wear resistance is very low and the coating was broken, exposing the aluminium metal beneath.

In contrast with this very thin conversion layer, very thick ceramic-like coatings may be applied to aluminium and titanium by a plasma electrolytic oxidation (PEO) process. The thickness of such a coating on aluminium may reach up to 100 µm [13], [17]. For space applications thicknesses in the range 10–30 µm would be of interest. Such a coating developed by 'Keronite' was screened in a first study. It not only offers no adhesion to steel AISI 52100, but it also did not peel off during fretting [18] (a later study has confirmed this; see section 3.4 in [19]). This is an advantage over anodised layers, where debris is produced that could contaminate other areas in the spacecraft.

Another frequently used alloy is **titanium alloy Ti6Al4V** (Ti6AV). Since titanium also has a high propensity to cold welding, several coatings were investigated. In a first study, only the disc was coated, while the Ti6AV pin was left uncoated. Here, all of the coatings were broken and adhesion was found before end of the test (5000 cycles). Moreover, no clear recommendation of soft or hard coatings can be made. The lowest adhesion values were found for Balinite B and a thin version of Keronite for titanium (6 µm), but also for the solid lubricant Dicronite DL5 (Fig. 13).

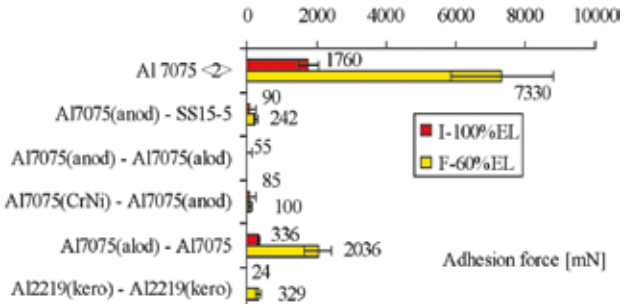

Fig. 12. Adhesion force of aluminium-based coatings under impact (I) and fretting (F) conditions. Adhesion between the Al parts is strongly reduced by hard anodising (anod), CrNi plating (CrNi), with no adhesion for (thick) Keronite [13],[18]. A single Alodine coating (alod) is not effective in preventing cold welding because of its low thickness <1 µm.

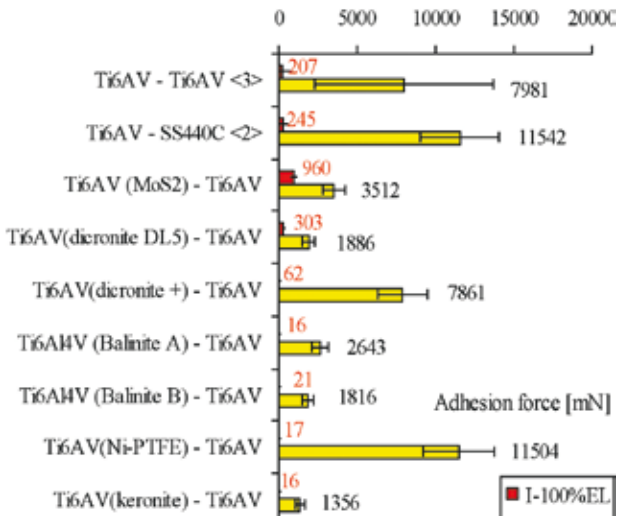

Fig. 13. Adhesion force of coatings on Ti6AV under impact (I) and fretting (F) conditions. Under impact, hard coatings prevented cold welding, but under fretting, all coatings were broken. The lowest adhesion forces were found for Ti6AV with thin (~6 µm) coatings of Balinite B and Keronite.

3.4 Thin and thick coatings under fretting and thermal cycling

From the results above, it can be seen that long-term fretting tests of hard coatings on soft substrate metals led in most cases to the failure of the coating. Examples include TiC on stainless steels [15], anodised aluminium alloys [12] and several coatings on Ti alloys [16]. For all these coatings one common parameter is their thickness, which is in the range of a few microns.

A dedicated set of studies was carried out to investigate whether thick coatings are more resistant to cold welding under fretting conditions. The 3G Keronite process can achieve thick ceramic coatings on soft metallic substrates. Based on plasma electrolytic oxidation (PEO), this is a relatively new, environmentally safe electrolytic coating process that can be applied to light metals such as Mg, Al, Ti and their alloys. This represents a rapidly developing sector in surface engineering. The process involves the use of higher voltages than in anodising, and the electrolyte usually consists of low-concentration alkaline solutions, and all variants of the process are considered to be environmentally friendly. The process results in the formation of ceramic layers up to 100 µm thick.

Therefore, coatings with thicknesses from 17 µm to 55 µm were applied to three aluminium alloys (AA2219, AA7075 and AA6082) that are widely used in spacecraft hardware. They were investigated for their resistance to cold welding under fretting before and after thermal cycling. As a counterpart, conventional bearing steel AISI 52100 was used. No adhesion was found and the coatings did not break. The coatings were then subjected to 20 thermal cycles between –185°C and +107°C, after which no cracking/delamination was detected. Finally, the fretting tests were repeated, and again the coatings survived without showing breakage, debris formation or adhesion [19].

Hence, 3G Keronite coatings ~20 µm thick on aluminium in contact with bearing steel do not show breakage of the coating or adhesion under fretting. On the other hand, Keronite coatings 6–10 µm thick on Ti alloy Ti6Al4V were found

to be insufficient to prevent cold welding. With Keronite in contact with itself or with Invar, breakage was observed and cold welding occurred. However, for Keronite in contact with itself with one additional layer of MoS_2 (PVD), no cold welding was found [20]. This study also considered thermal cycling, even down to liquid helium temperature, but upon metallographic inspection, and after second fretting tests, no degradation due to thermal cycling was found.

These studies indicate that thick Keronite coatings (>17 µm) offer significantly enhanced resistance against cold welding under fretting, and are *not* degraded by thermal cycling. The role of MoS_2 coatings (resin-bonded or PVD) on Keronite still has to be investigated in more detail; in some cases no additional benefit has been found, but at least no drawbacks are known yet [20], [19].

3.5 Surface morphology after impact and fretting

Impact and fretting can result in considerable changes in material surfaces. After impact testing, a SS17-7PH pin shows plastic flow, which can be seen by the piling up at the edges of the pin's contact area (Fig. 14a). On the other hand, fretting of SS17-7PH steel in contact with itself shows strong surface destruction due to adhesive wear. Material is torn out of the surface, and is pressed back or adheres to the contact partner (Fig. 14b).

As mentioned above, MoS_2 coating on SS17-7PH could not prevent cold welding. The lubrication effect of the coating was lost after 20 cycles (200 seconds fretting, 42 000 strokes), and adhesion up to 5870 mN was later found. Figure 15 shows strong surface destruction of the MoS_2-coated disc, which is similar to that found on the uncoated disc. EDX distribution of Mo taken from the disc shows that no Mo was present in the contact area after 7000 cycles. Both pin and disc show fretting wear scars similar to those found on discs without MoS_2 coating.

In contrast with all the coatings investigated so far, the thick Keronite coating on Al AA2219 was the only one that prevented adhesion and which was not destroyed under fretting conditions. Hard anodising of Al AA 7075 prevented adhesion, but much loose debris was found (Fig. 16).

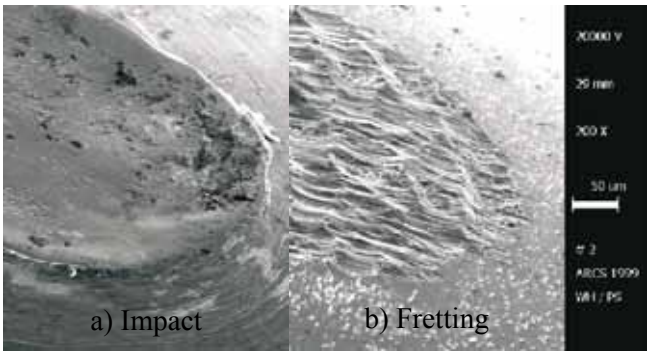

Fig. 14. Surface of a pin (SS17-7PH) after impact and fretting. (a) Some plastic flow is visible from the piling up of edges. (b) Strong destruction of the surface, adhesive wear combined with high adhesion forces (compare with Fig. 10 for adhesion forces: 'SS17-7').

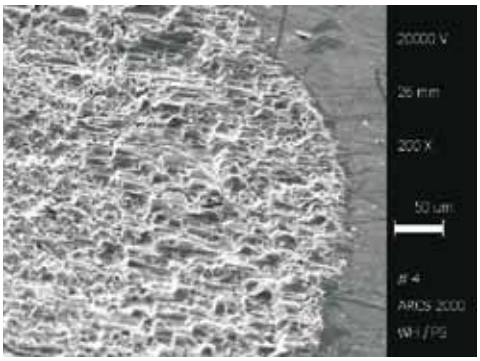

Fig. 15. Surface of disc of SS17-7PH with MoS_2 coating after fretting tests (compare with Fig. 11 for adhesion forces). The lubrication effect was lost after fretting movements lasting less than 20 s (confirmed by EDAX mapping; no Mo was present in the contact area).

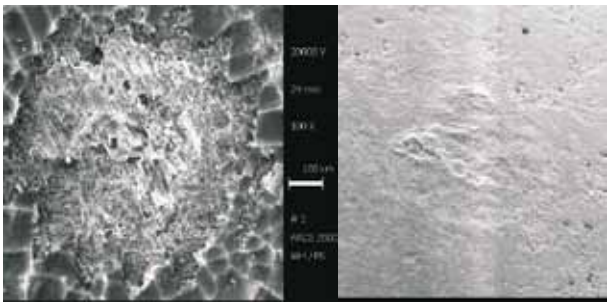

Fig. 16. Comparison of Al coatings under fretting. *Left*: The hard anodising on Al7075 was broken. *Right*: The Keronite coating on Al AA 2219 shows no fretting marks (compare with Fig. 11 for adhesion forces).

3.6 Influence of contact parameters under fretting / theoretical prediction of adhesion forces

3.6.1 Background – influence of impact contacts

Basic studies [11] at AIT have shown that under impact conditions, an increase in the static load leads to an increase in the adhesion force. Figure 17 shows the adhesion forces found for stainless steel SS17-7PH in contact with itself (ball on flat contact, without any coating). The three bars refer to the measured adhesion forces under static loads related to contact pressures of 40%, 60% and 100% EL. It can be seen that the adhesion force increases with contact pressure when impact occurs (no fretting).

On the other hand, studies investigating adhesion under fretting have shown severe wear (see above). Impact leads only to some plastic deformation, leading to adhesion forces no higher than 2 N. Fretting, however, causes severe surface damage, sometimes leading to adhesion forces several times greater than 10 N. Hence, for fretting this influence must be assessed separately.

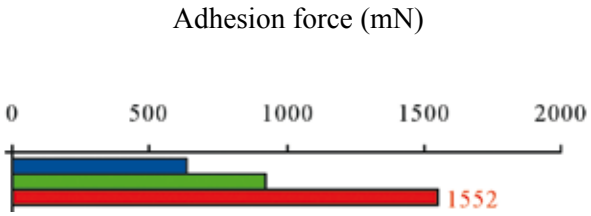

Fig. 17. Adhesion force (in mN) of steel SS17-7PH in contact with itself (uncoated) under impact. The adhesion increases with static loads related to contact pressures of 40%, 60% and 100% EL.

3.6.2 Definition of the contact area

Up to now, the influence of 'material' on adhesion forces has been discussed. But cold welding depends not only on the material, but also on the geometry, namely, the contact area. The macroscopically measureable adhesion force is defined on the following basis. The ultimate yield strength (of the softer material) times the 'real clean contact area'. Here, the latter is generally unknown, unpredictable and orders of magnitude smaller than expected. In the following we describe (1) the nominal contact area, (2) the 'real contact area' and (3) the 'real clean contact area'.

1. **Nominal contact area.** As is typical for tribological contacts in mechanisms, only the nominal contact area is known. In flat-to-flat contacts the nominal contact area is obvious, but in ball-to-flat-contacts it may be calculated using Hertzian theory, assuming the contact to be within the elastic regime.

2. **Real contact area.** Due to surface roughness, the full contact area does not come into contact, but only the tips. Of course the difference between nominal and real contact areas is influenced by mechanical and surface properties. In general, the real contact area is orders of magnitude smaller than the nominal one. There are several ways to estimate this real contact area. A simple analytical way to estimate the real contact area is to divide the load by the yield strength of the material in question [7]. Modern computational tools may be used to simulate real contact areas using 3D topographies and mechanical data, although this is still only practicable for static contacts. Including motion leads to increased computational efforts.

3. **Real clean contact area.** In order to calculate adhesion forces, one more reduction step is necessary; again only a part of the real contact area contributes to adhesion. As mentioned above, surfaces are covered by natural contaminant layers. Especially, chemical reaction layers prevent cold welding. If the tips of two rough bodies come in to contact, both of these layers must be broken in order to enable a metal–metal contact. Only these single joints between the clean metal surfaces are welded, and the adhesion force is the sum of all these single welded joints. It is this last contribution that cannot be predicted by simulation.

Hence, it must be anticipated that a theoretical prediction of adhesion forces is not possible. Moreover, in the case of fretting, wear would also have to be considered, since it changes the surface topography and the contact area. A study was therefore undertaken to investigate these theoretical and experimental approaches [6].

3.6.3 Determination of adhesion forces: three approaches (models and experiment)

The objective of this study was to investigate whether the contact pressure and contact area have an influence on the adhesion force under fretting conditions.

A set of four test parameters was selected with varying loads and pin radii (i.e. curvature of a spherical pin tip; see Table 1). Three tests were carried out at a load of 1 N with pin radii of 1 mm, 2 mm and 15 mm, and related to contact pressures of 118%, 57% and 19% EL. One test was made with a similar contact pressure of 58% EL, but using a different combination of radii (10 mm) and a load of 12 N (see Table 1). For all the tests, the same material combination was selected: AISI316L in contact with itself without any coating. This is a stainless austenitic steel that has been tested previously and shows high adhesion forces. Three parallel tests were carried out for each set of parameters. For material properties, see the table in Annex C. The contact pressures were calculated using standard Hertzian theory (see e.g. [9]).

3.6.3.1 Theoretical estimation of adhesion forces (approach 1: 'theory')

Theoretically, the adhesion forces can be calculated on following basis: the ultimate yield strength times the contact area. The contact area of a ball-to-flat contact is calculated using Hertzian theory, based on which the adhesion forces in a ball-to-flat contact should decrease when using a smaller contact area. The values for the stainless steel AISI316L in contact with itself are shown in Fig. 18, from which it can be seen that the (theoretical) adhesion force is directly related to the contact area (Table 1).

3.6.3.2 Estimation of adhesion forces using fretting wear area (approach 2: 'semi-theory')

A second way to predict adhesion forces is based on experimentally derived contact areas: the wear contact area measured after a friction test times the yield strength. The results are shown in Fig. 19. Here, the contact areas measured after the fretting tests were multiplied by the yield strength.

3.6.3.3 Results from fretting experiments (approach 3: 'experiment')

Three parallel tests were performed for each set of parameters; the average values for each set are shown in Fig. 20. Adhesion forces are generally high, as expected for this material. The only significant difference is seen for the smallest contact area (pin radius 1 mm at 1 N), where the adhesion force is slightly lower (6.2 N).

Table 1. Test parameters: three parallel tests per set.

Tests	Tip radius (mm)	Load (N)	Contact pressure (MPa)	Contact pressure (% EL)	Contact area (mm^2)
F1x	1	1	1272	118	0.0012
F2x	3	1	611	57	0.0025
F3x	10	12	209	58	0.0287
F5x	15	1	627	19	0.0072

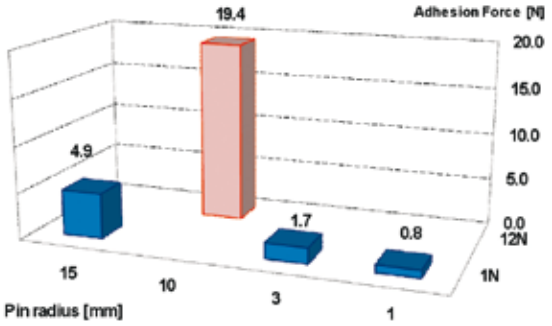

Fig. 18. Adhesion forces calculated using the yield strength times the Hertzian contact area.

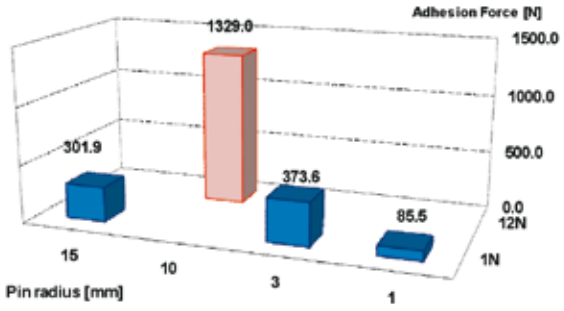

Fig. 19. Adhesion forces calculated using the wear contact area (the contact area measured after the fretting test) times the yield strength.

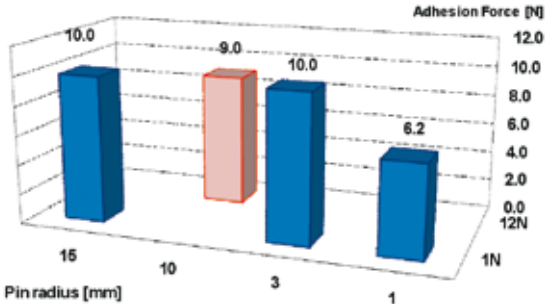

Fig. 20. Adhesion forces: measured values (average values of three parallel tests, uncertainty of test method 30%).

On the other hand, fretting wear leads to an increase in the contact area. In the test with the higher load, the contact area is significantly higher than in the others. Hence, the wear is greater with higher loads, even with comparable contact pressures: ~58% EL for a radius of 10 mm and load of 12 N, and a radius of 3 mm and load of 1 N.

3.6.4 Comparison of modelling and experimental results from fretting

The adhesion under fretting was derived using three methods:

1. **Theory:** calculating the Hertzian contact area times the yield strength would lead to the conclusion that smaller radii are preferable. Neglecting any wear, Hertzian theory gives a smaller contact area, and the resulting adhesion force is correspondingly lower (Fig. 18).

2. **Semi-theory:** yield strength times measured wear contact area, i.e. using the wear contact area measured after a fretting test (Fig. 19). The derived values of the adhesion force are similar to those obtained using method 1. The conclusion would be similar: use a smaller radius. Even though the contact pressure is higher than the EL, the wear does lead to a smaller contact area when the tip radius is smaller. However, starting with contact pressure higher than EL is still not an issue.

3. **Experiment:** the measured adhesion forces are comparable for all parameter sets. They show no significant influence of initial contact details (Fig. 20). A smaller contact radius seems to be advantageous, and the adhesion force is slightly lower (average 6.2 N compared with approximately 10 N for all other tests).

It is clear that neither the theoretical nor the semi-theoretical extrapolations fit the observed experimental behaviour. The main reason is the fact that the definition and determination of the ‘contact area’ are insufficient. The theoretical approaches reveal a ‘nominal contact area’, but the adhesion is related to what can be referred to as the ‘real contact area’.

The real contact area, i.e. the area where metallic bonds actually exist, is much smaller than the nominal one predicted by theory. This is due to the surface roughness and surface contamination, both of which reduce the measured adhesion forces by orders of magnitude (compare Figs. 19 and 20). Using the theoretical approaches, the highest adhesion should be found at a load of 12 N (Figs. 18 and 19). Even this overall tendency is not found in experimental tests (Fig. 20). Wear due to fretting is levelling out the contact pressure to values in the range of few Megapascals.

Hence, the adhesion forces cannot be ‘modelled’ since neither the ‘real contact area’ nor fretting wear can be predicted.

4 The ‘cold weld data’ database

4.1 Database inputs

Several studies of cold welding using different material combinations have been performed in recent years. They were all performed in accordance with the ARCS in-house standard approved by ESA [5] and are therefore regarded as being comparable (tests done within separate projects or customer projects are not included in the database). For each test a data sheet was generated within the related call-off order. Based on all the tests performed, individual data sheets were generated (see Fig. 21), collected together and can now be accessed online [21].

4.2 Classification of adhesion forces in the database

The data sheets have been included in the database, and summary tables created showing for which combinations of materials data are available. The database also includes a classification of adhesion forces at four levels (Table 2). Electronic versions of these data sheets can be accessed online.

Based on the results of ‘general validation studies’, the database includes:

- data that are fully comparable based on test parameters related to material properties
- data covering the contact modes ‘impact’ and ‘fretting’
- summary tables showing the material combinations for which data are available, and a classification based on the severity of adhesion
- a detailed data sheet for each test.

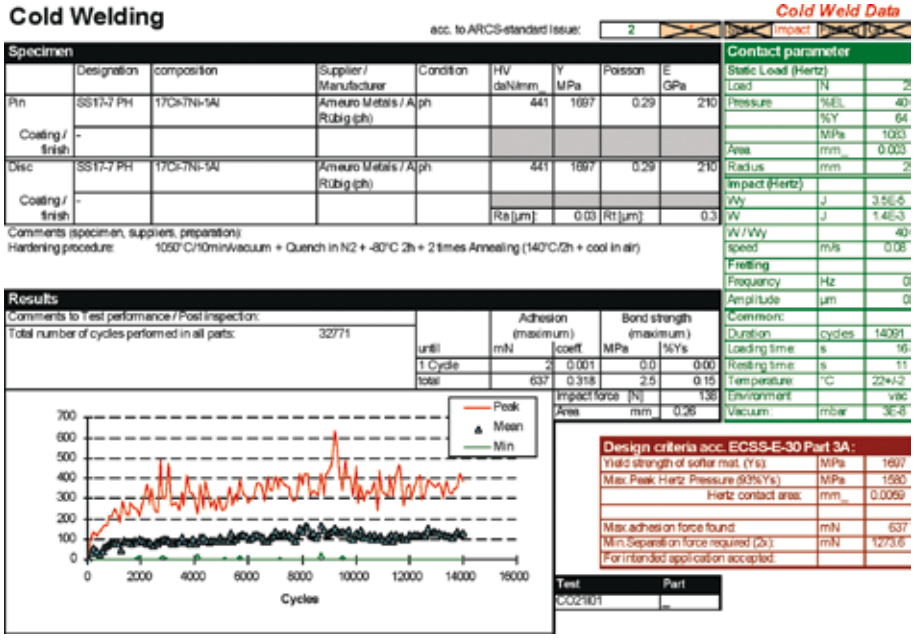

Fig. 21. Data sheets generated for all cold welding tests carried out in accordance with the ARCS in-house test method [5] are available online.

Symbol	Adhesion force (mN)		Comment on adhesion	Comment on Use
	Lower limit	Upper limit		
●	0	200	No or negligible adhesion, noise of test	Use recommended
◑	201	500	Small, measureable adhesion	Security measures to be undertaken
◔	501	5000	Strong adhesion	Direct use not recommended
○	5001	higher	Severe adhesion	Direct use not recommended

Table 2. Classification of adhesion forces used in the database.

Related documents include:

- the ARCS in-house specification describing the test method
- sample dimensions and derivation of test parameters
- a summary of each test divided into fretting and impact
- detailed data sheet for each test that can be opened by clicking on the relevant symbol.

The summary (or so-called survey) tables are based on the classification of adhesion forces found in different material combinations as shown in Table 2.

4.3 Accessing and using the online database

The database can be accessed at the website of the Austrian Institute of Technology:
www.advanced-materials.at/products/products_AAC_Produkte_SpaceTesthouse_en.html

but also directly at
http://service.arcs.ac.at/coldwelddata/

This ‘cold weld data’ database contains links to two survey tables, one for fretting and one for impact. These tables will be periodically updated as future test result data become available.

In the example of a table for fretting shown in the screenshot below, the classification provides basic information on the cold welding tendency of a certain combination of materials. The table shows the actual knowledge and the availability of test data: an empty field means that no data are available. The symbols indicate the level of adhesion found in the test. A click on the symbol opens a detailed data sheet that includes all information on the materials, the test parameters, the main results and the test number (as a tracking code).


Cold Weld Data
Space Materials
Home
About Coldwelding
Table Fretting
Table Impact
Contact
User login
Cold welding under vacuum due to Impact or Fretting
AUSTRIAN RESEARCH CENTERS

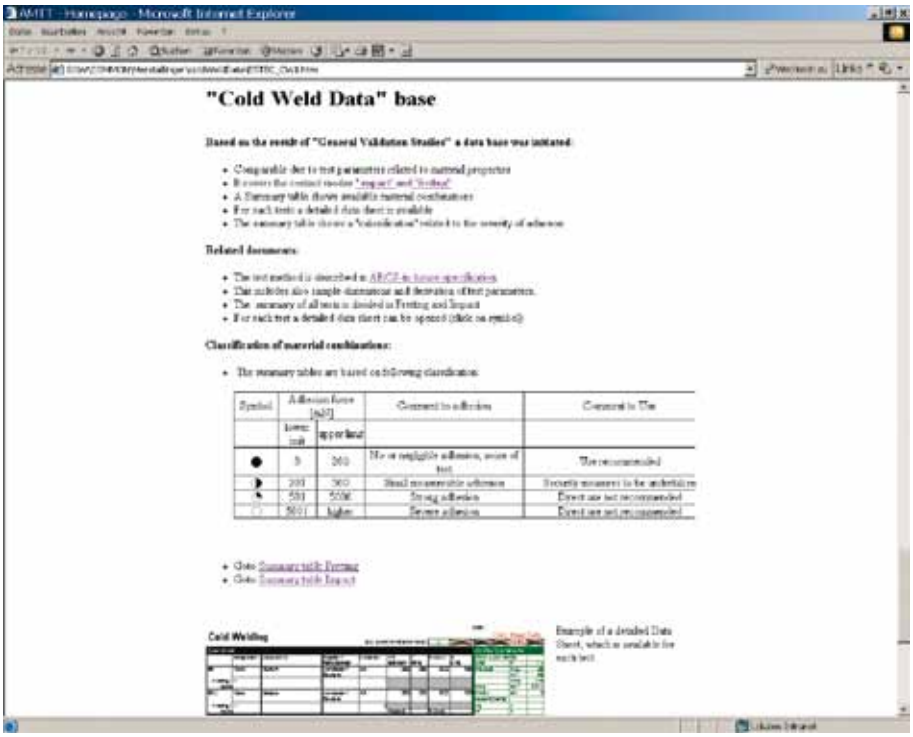
"Cold Weld Data" base
Related documents:
Classification of material combinations:
Cold Welding

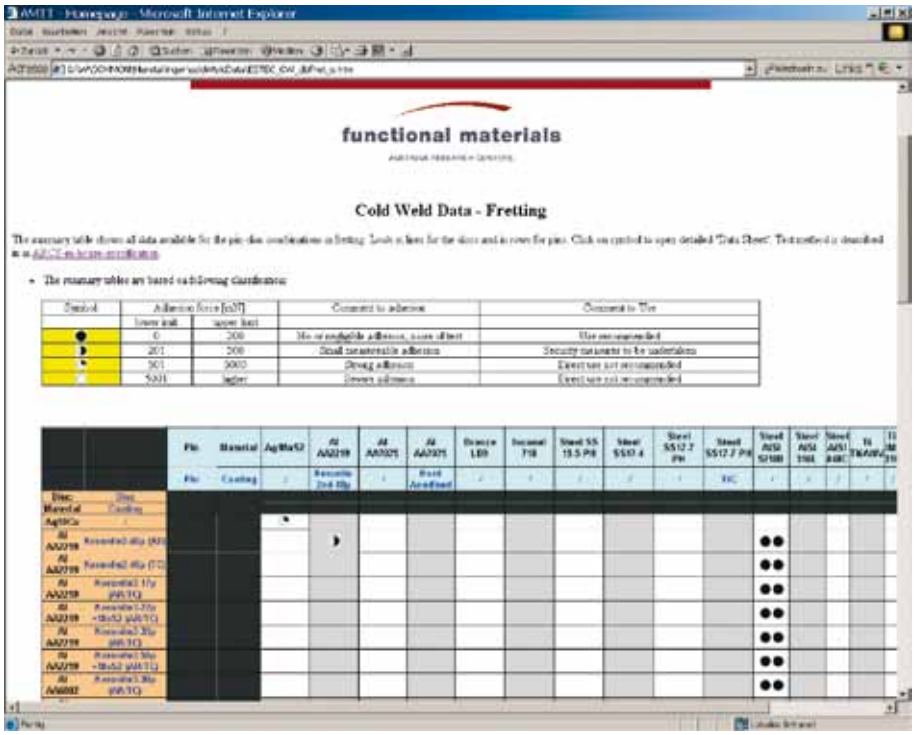
functional materials
Cold Weld Data - Fretting

5 Conclusions

1. Test equipment (Annex A) and a test method (Annex B) have been developed to study the cold welding of material interfaces that make contact under impact and fretting conditions. The method and the results represent a step forward in studies of cold welding effects from 'common experience' to measurable data that will be useful for designers of spacecraft applications.

2. In order to provide engineers with the experimental data, AIT has set up an online database that aims to bring together all the data generated from all studies performed for ESA and industry. The database can be accessed free of charge after registration: *http://service.arcs.ac.at/coldwelddata.*

3. It has been shown that the **theoretical predictions are by no means comparable with experimental** data. The main reason is that the adhesion force is driven by the 'real contact area', which can not be predicted. Hertzian theory would predict a 'nominal contact area', neglecting surface roughness and surface contamination. The latter in particular is the main contributor and remains unpredictable.

4. A wide range of material combinations, including metal–metal (SS17-7PH in contact with itself and Al alloy AA 7075 in contact with itself), metal–polymer (SS17-7PH versus Vespel SP3), as well as several coatings on steel, aluminium and titanium have been investigated under impact and fretting conditions. The data can be found in Annex C. These results and those of future work are now searchable online.

5. Tests have revealed that the **range of adhesion** forces in uncoated metal–metal contacts with typical engineering surfaces and without coatings **depend on the type of contact**:

   – in static contact, adhesion forces were below 0.5 N,
   – under impact, adhesion forces were up to 2 N, and
   – under fretting, adhesion forces in excess of 18 N were found.

   Basic material physics (type of atomic bonds) indicate that no technically measurable adhesion between metals and polymers and ceramics can be expected. A few tests on steel or aluminium and polyimide have not contradicted this premise.

6. In order to **avoid cold welding,** polymers or ceramics can be selected, but these materials may not be suitable for space hardware and mechanisms. Hence, metal–metal contacts often cannot be avoided. In that case, in order to reduce the risk of cold welding, the first strategy would be to use **dissimilar alloy pairs**, e.g. stainless steel versus hard steel (low adhesion is likely). The second strategy would be to apply coatings, although here the type of contact and the substrate material need to be well known.

7. Under **impact**, hard coatings on **stainless steel** (TiC, for instance) may break, so that although the risk of adhesion is lower, it is still present. Soft coatings made of solid lubricants (e.g. MoS_2) can repair themselves during impact, so they are more effective in preventing adhesion than hard

coatings. Stainless steels are generally too soft to support hard coatings under impact conditions. Hard anodised **aluminium** can withstand impact. **Titanium** alloys must be coated with hard coatings to resist cold welding if only impact is expected.

8. Under **fretting** conditions, none of the investigated coatings on stainless steel (SS17-7PH) is able to prevent cold welding. Also MoS_2 is not effective under fretting, and the lubrication is quickly lost. Hence, the best strategy must be to use different steels (maximum one of which should be austenitic). Hard coatings should not be used on hard steels. In contrast with steel, hard anodising of **aluminium** prevents adhesion under fretting conditions, but much loose debris is formed. A thick 'Keronite' coating (20 μm), which is based on a plasma-electrolytic oxidation (PEO) process, is not only resistant to fretting but also avoids debris formation. A test using an uncoated **titanium** pin against coated titanium discs did not provide a 'general solution'. All thin coatings – solid lubricants and hard coatings – were destroyed in the fretting contact. The best combinations still showed medium adhesion after breakage of the coating. The combination titanium and low-adhesion steel also did not provide a solution. Further research will target thick coatings produced by PEO (Keronite).

References

[1] European Cooperation for Space Standardization (ECSS) ECSS-E-ST-33-01C (2009), 'Mechanisms', section 4.7.5.4.5 'Separable contact surfaces'.

[2] Merstallinger, A. & Semerad, E. (1995). *Tribological Properties of Ga3Z1*. ESTEC Contract no. 8198/89/NL/LC, WO 32.

[3] Johnson, M.R. (1989). *The Galileo High Gain Antenna Deployment Anomaly.* California Institute of Technology, Jet Propulsion Laboratory (JPL), Pasadena, CA.

[4] Merstallinger, A., Semerad, E., Dunn, B.D. & Störi, H. (1995). *Study on Cold Welding under Cyclic Load and High Vacuum.* 6th European Space Mechanisms and Tribology Symposium, Zürich, Proceedings ESA SP-374.

[5] Merstallinger, A. & Semerad, E. (1998). *Test Method to Evaluate Cold Welding under Static and Impact Loading*. In-house standard by ARCS approved by ESA, Issue 2. Uncertainty Evaluation for 'Test Method to Evaluate Cold Welding under Static and Impact Loading', in-house standard by ARC Seibersdorf Research GmbH, Issue 2, audited in 2003.

[6] Merstallinger, A., Sales, M., Semerad, E. & Dunn, B.D. (2009). *Reduction of Cold Welding by Geometric Parameters.* Proc. 13th European Space Mechanisms and Tribology Symposium, Vienna, ESA-SP-670 (ESTEC Contract no. 11760/95/NL/NB, CO65).

[7] Roberts, E. (2001). *Space Tribology Handbook*. ESTL, AEA Technology.

[8] Merstallinger, A., Semerad, E. & Dunn, B.D. (1997). *Cold Welding due to Fretting under Vacuum, Helium and Air.* Proc. 7th European Space Mechanisms and Tribology Symposium, ESTEC, Noordwijk, the Netherlands.

[9] Johnson, K.H. (1985). *Contact Mechanics*. Cambridge University Press.

[10] Persson, U., Chandrasekaran, H. & Merstallinger, A. (2001). Adhesion between Some Tool and Work Materials in Fretting and Relation to Metal Cutting. *Wear* **249**, 293–301.

[11] Merstallinger, A., Semerad, E. & Dunn, B.D. (1999). *Influence of Impact Parameters and Coatings on Cold Welding due to Impact under High Vacuum.* Proc. 8th European Space Mechanisms and Tribology Symposium, Toulouse, France (ESTEC Contract no. 11760/95/NL/NB, CO 12, 1998).

[12] Merstallinger, A., Semerad, E., Scholze, P. & Schmidt, C. (2001). *Screening of Contact Materials for Cold Welding due to Fretting.* ESTEC Contract no. 11760/95/NL/NB, CO20, Materials Report 3150.

[13] Shrestha, S., Merstallinger, A., Sickert, D. & Dunn, B.D. (2003). *Some Preliminary Evaluations of Black Coating on Aluminium AA2219 Alloy Produced by Plasma Electrolytic Oxidation (PEO) Process for Space Applications.* Proc. 9th International Symposium on Materials in Space Environment (ISMSE), ESTEC, Nordwijk, the Netherlands.

[14] Merstallinger, A., Semerad, E., Scholze, P. & Schmidt, C. (2000). *Influence of Coatings on Adhesion under Impact*. ESTEC Contract no. 11760/95/NL/NB, CO21, Materials Report 2663.

[15] Merstallinger, A., Semerad, E. & Costin, W. (2004). *Influence of Steel Types on Cold Welding under Fretting and Impact.* ESTEC Contract no. 11760/95/NL/NB, CO40.

[16] Sales, M., Merstallinger, A., Costin, W., Mozdzen, G. & Semerad, E. (2006). *Influence of Titanium Alloy Ti6Al4V on Cold Welding under Fretting and Impact*. ESTEC Contract no. 11760/95/NL/NB, CO52.

[17] Shresta, S. & Dunn, B.D. (2007). Advanced Plasma Electrolytic Oxidation Treatment for Protection of Lightweight Materials and Structures in Space Environment. *Surface World*, November, 40–44.

[18] Merstallinger, A., Semerad, E. & Costin, W. (2002). *Assessment of Keronite for Cold Welding and Friction*. ESTEC Contract no. 11760/95/NL/NB, CO39, Metallurgy Report no. 3522.

[19] Sales, M., Merstallinger, A., Shresta, S. & Dunn, B.D. (2008). *Combating the Fretting Wear and Cold Welding of Aluminium Alloys on Spacecraft Hardware using the Plasma Electrolytic Oxidation (PEO) Process.* 22nd International Conference on Surface Modification Technologies (SMT22), Tröllhättan, Sweden. ESTEC Contract no. 11760/95/NL/NB, CO60.

[20] Sales, M., Merstallinger, A., Shresta, S. & Dunn, B.D. (2009). *The Fretting Wear Behaviour of Plasma Electrolytic Oxide Coatings on Aluminium Alloys.* Proc. 11th International Symposium on Materials in Space Environment (ISMSE), Aix-en-Provence, France. ESTEC Contract no. 11760/95/NL/NB, CO72.

[21] Sales, M., Mozdzen, G., Merstallinger, A., Semerad, E. & Costin, W. (2008). *Cold Welding Summary Chart Collection of Data of all Performed Studies*. ESTEC Contract no. 11760/95/NL/NB, CO53.

Materials: abbreviations and data

Explanations of the material abbreviations used in this publication, and the data used to calculate the test parameters, are shown in Table 3.

Table 3. Materials: abbreviations and data

Abbreviation	Designation	Composition	Condition	H_V (daN/mm²)	Yield (MPa)	Poisson	E (GPa)
Al7075	Al alloy Al AA 7075	2.1–2.9Mg1.2–1.6Cu0.18–0.28Cr5.1–6.1Zn	T7351	170	654	0.33	72
Bronze LB9	Bronze LB9 BS 1400 LB4	Cu–4–6Sn–8–10Pb–2Zn–0.25Fe–0.01Al–0.2Mn–2Ni–0.5Sb–0.1S	AR	160	130	0.34	80
SS15	Stainless steel SS15-5PH	14–15.5Cr3.5–5.5Ni0.15–0.45Nb<0.07C2.5–4.5Cu	H1025	393	1000	0.27	196
440C	AISI 440C	Fe–1.01C–0.47Si–0.56Mn–0.014P–<0.002S–17.81Cr–0.27Ni–0.48Mo	Harden	700	2692	0.283	200
SS17	Stainless steel SS17-7PH	17Cr–7Ni–1Al	PH	441	1697	0.29	210
Ti834	Ti-IMI 834	Ti5.8–Al4Sn–3.5Zn–0.7Nb–0.5Mo–0.35Si–0.06C	AR	334	1285	0.32	112
Ti6AV	Ti-IMI 318	Ti6Al4V	AR	338	850	0.32	105
Vespel SP3	Vespel SP3	85Pl–15MoS_2	AR	18	68	0.41	2.5
$AgMoS_2$	Ag/MoS_2	Ag 15 vol% MoS_2	AR	26	138	0.367	71
Ag10Cu	Ag10Cu	Ag10Cu	AR	150	620	0.367	82.7
Inconel718	Inconel718 / ASTM B 637)	Fe–53.6Ni–18.9Cr–5.3Nb–3Mo–0.98Ti–0.03C–0.13Si–0.12Mn–0.008P–0.001S–0.49Al–0.2Co–0.06Cu–0.004B	AR	348	1338	0.25	211
SS316L	AISI 316L	Fe–0.011C–0.41Si–1.42Mn–0.031P–17.3Cr–11.2Ni–2.09Mo–0.05W–0.098Co–0.041V–0.026S	Austenitic	175	675	0.28	190
52100	AISI 52100 (SKF)	Fe–1C–0.3Si–0.4Mn–0.03P–0.03S–1.6Cr–0.3Ni–0.3Cu	AR	700	2692	0.28	200
AL 2219	AL AA 2219	6.3Cu–0.3Mn–0.18 Zr–0.1V–0.06Ti	T851	138	531	0.33	73.8

Annex A: Description of test devices

A.1 Cold welding: impact and fretting

This unique, highly specialised equipment allows simulations of cyclic closed contacts such as those found in relays, or at end stops, and measurements of the forces necessary to re-open the contact, i.e. the adhesion forces. This effect is referred to as 'cold welding', but other terms such as stiction may also be used. Two facilities cover the most dangerous types of contact: impact during closing and fretting within the closed contact. The latter facility may also be adapted to fretting wear tests.

The aim of the test is to provide designers and engineers with data on adhesion forces that have to be considered in design of mechanisms, in order to assess, on the one hand, cold welding on bare metal contacts and, on the other, the performance of coatings in preventing adhesion. If no specific parameters are demanded, the tests are performed in accordance with the ARCS in-house specifications, thus enabling comparison of the results for different material pairings, and the collection of data in a database. Considerable efforts have been made to offer special competence in cold welding effects.

Cold welding (1): Impact test facility

The impact test facility (Fig. A.1), for loads up to 100 N, enables the measurement of adhesion forces under vacuum between contact points after cyclic contacts, varying from static contacts (long-term compression) to slow closing cyclic contacts (static adhesion), and after impacts with impact energies up to 0.02 J.

The impact test facility, which was designed and developed in-house, consists of an UHV system (10^{-8} mbar after bake-out at 130°C) with an ion getter pump and an air damping system for vibration-free measurements. Emphasis

Fig. A.1. Impact test facility (inside view).

was given to the universality of the test setup, which covers a wide range of impact energies, contact pressures and contact times.

The contact is made between a ball and a flat disc. The ball is mounted on a pushrod, which is driven by an electromagnet. A low-friction loading system enables an accuracy of 1 mN (0.1 g) for the adhesion force measurement, which is made directly above the pin in the vacuum chamber using a piezo force transducer. The transducer measures the impact force as well as the adhesion, i.e. the force needed to separate the two materials.

Cyclic loading may be done either slowly (‘static’) or by impact (‘dynamic’) with defined energies that are determined by the mass of the pushrod and its velocity at impact, as measured by a distance sensor. The impact energy, the impact force, the contact duration, the load during contact and the separation are controlled by computer. By varying the ball radius (typically 2–20 mm), the contact pressure can be adjusted to the yield strength of most materials. As an option, the contact surfaces can be cleaned in situ by glow discharge before the test. The surface roughness is characterised by profilometry.

The above test methods are adequate to detect the propensity to cold welding at an early stage. They are capable of assessing the statistical spread with increasing contact cycles in order to see if there is a tendency to cold welding or single catastrophic failure.

Cold welding (2): Fretting test facility

The fretting facility (Fig. A.2) allows investigations of the influence of fretting on the tendency to cold welding of materials. After a certain number of fretting cycles the adhesion force between contacts is measured.

The loading mechanism is similar to that of the impact test device described above. The loading and adhesion forces are measured by the *z*-direction of a 3-axis piezo transducer mounted directly below the disc under vacuum. The friction force due to the fretting movement is measured in the *x*-direction. The fretting movement (sine, triangle or square wave) is generated by a piezo actuator for frequencies between 0 and 300 Hz and amplitudes up to 100 µm. This lateral movement is transduced to the pin via a CuBe plate and controlled at the contact by a triangulation sensor.

This facility has allowed for the first time the simulation of high-frequency vibrations resulting from bearings, for example, combined with measurements of the adhesion force.

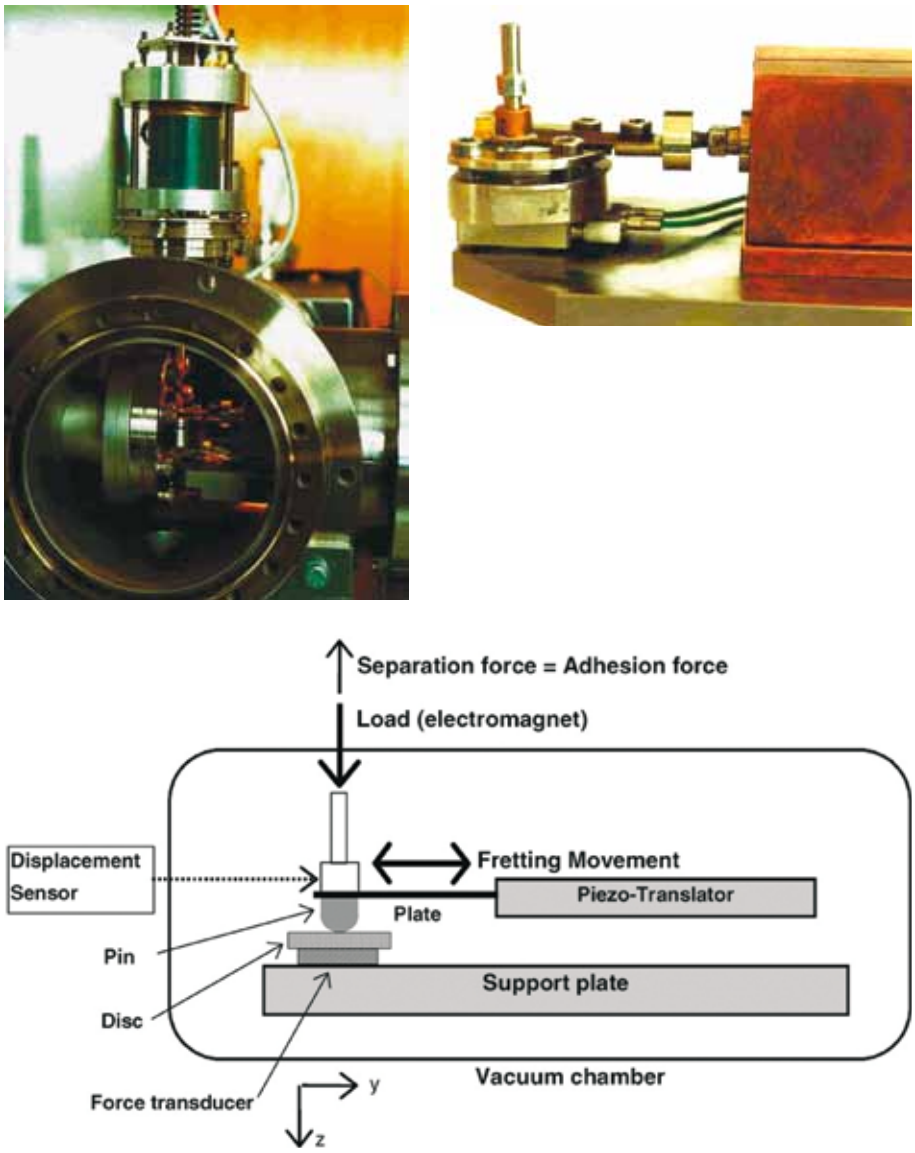

Fig. A.2. Fretting facility: device (*top left*); inside view (*top right*); functional sketch (*bottom*).

A.2 Topographic analysis (profilometry)

The topography of a surface may be analysed by two means: by determining the surface 'roughness', or by measuring holes or the volume of balls removed after friction tests.

The **surface roughness** can be measured and evaluated using a computer-controlled **stylus profilometer** (Rank Taylor Hobson Surtronic 3+). Based on international standards, all typical surface parameters in any kind of profile investigation (such as determination of the cross-sectional area of wear tracks) may be calculated using Windows-based software. The maximum size of samples needed is 10 × 40 mm, which is valid for the roughest surfaces. For finer surfaces, smaller samples can be used. Curved specimens may also be investigated (the dimensions have to be defined in detail). It is also possible to determine the surface roughness inside holes or tubes (with a minimum diameter of 8 mm).

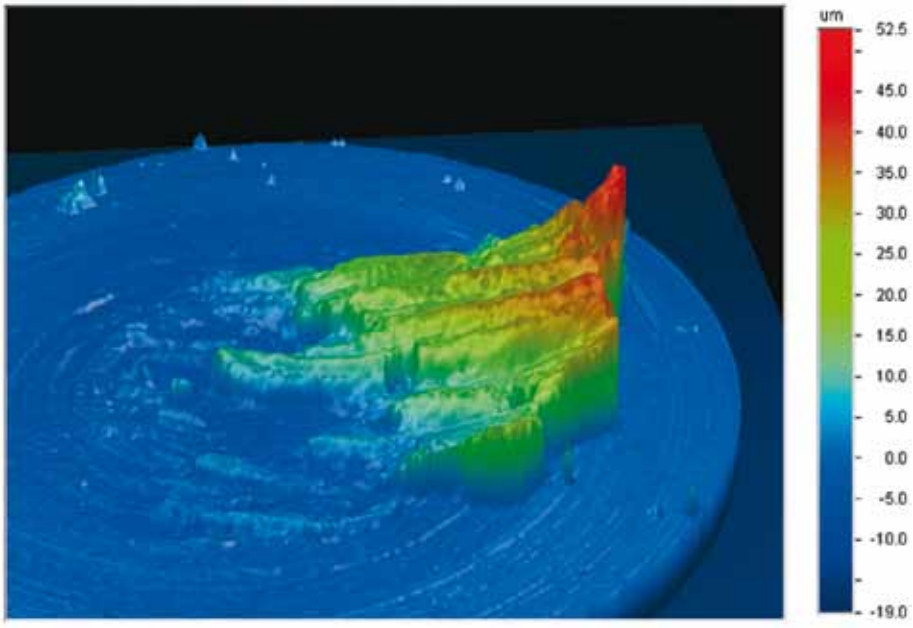

Fig. A.3. Example of a ball after a friction test.

For more general assessments of **3D surface topography,** a new **optical profiler** (Veeco NT1100) is used primarily to determine the dimensions of surface structures. Examples include measurements of the lost volume on discs after friction tests, or of a ball after a friction test.

The profilometer provides 3D topography, together with macros to calculate wear volumes on flat, as well as on spherical and cylindrical surfaces. Scanning areas range from 0.3 × 0.2 mm to 5.0 × 3.8 mm. The highest resolutions are 0.5 × 0.5 µm lateral and <0.1 nm vertical. The vertical scanning range may reach up to 1 mm.

In addition, all typical roughness parameters may be calculated. At present, however, no international standards are available, so the reproducibility of these values is not proven.

The Veeco NT1100 optical profiler can also be used to measure **wear volumes**. Figure A.3 shows an example of a ball after a friction test, where the original spherical surface of the ball has been subtracted. The remaining peak refers to the net volume of material sticking to the ball, which can be calculated.

Annex B: Proposal for a test method (in-house standard)

Abstract

This specification describes a test to determine the cold welding tendencies of materials and/or coatings intended for use in all types of contacts that are cyclically closed and opened. Simulations of such contacts include static or impact loading as well as subjecting the contacts to fretting, i.e. micro-vibrations in the direction of the contact plane. Cold welding is assessed by measuring the separation force in the vertical direction, referred to as the adhesion force.

This specification has been used to set up a database on cold welding for common material and coating pairings.

B.1 Scope

This specification describes a test to determine the cold welding tendencies of materials and/or coatings intended for use in all types of contacts that are cyclically closed and opened. Simulations of such contacts include static or impact loading as well as subjecting the contact to fretting, i.e. micro-vibrations in the direction of the contact plane. Cold welding is assessed by measuring the separation force in the vertical direction, referred to as the adhesion force. This includes deployment or end-stop mechanisms. This test is able to demonstrate the reliability of an opening device in accordance with the section on cold welding in the ‘Space Mechanisms Standard Requirements Specification’.

This specification has been used to set up a database on cold welding for common material and coating pairings.

B.2 General

B.2.1 Introduction

Repeated loading and unloading of contacts results in the destruction of oxide layers on the surface, which leads to increasing adhesion between the two surfaces, especially metals. Adhesion forces were found to increase in the order static contact, impact contact and fretting during static contact [B1]. Under fretting conditions at low loads, the adhesion can even exceed the load force.

Due the fact that the opening is done by some kind of spring with limited tension, the mechanism fails if the adhesion force exceeds the tension. This may be much less than the adhesion force, which is commonly related to cold welding in the sense of a real weld.

With this test method it is possible to assess the cold-welding tendency of a combination of two materials with or without coatings. To avoid alignment

influences, the contact is made between a pin with a spherical tip and a (flat) disc. The contact is closed and opened several times, referred to as 'cycles'. During each unloading, the force necessary to separate them in the vertical direction, i.e. the adhesion force,[1] is measured. Thereby, the maximum adhesion force is evaluated for a definite contact condition. The effect of surface cleanliness on the adhesion force may be simulated by applying a glow discharge (GD) cleaning process *in situ* directly before closing the contact.

The test parameters have been used to set up a database that will provide designers of space mechanisms with data on adhesion/cold welding.

B.2.2 Related documents

Some or all of the contents of the following documents is relevant to this specification:

ESA PSS-01-20: Quality assurance requirements for ESA space systems.

ESA PSS-01-70: Materials, mechanical parts and process selection and quality control for ESA space systems.

ESA PSS-01-201: Contamination and cleanliness control.

ESA PSS-01-700: The technical reporting and approval procedure for materials, mechanical parts and processes.

ESA PSS-01-738: High-reliability soldering for surface-mount and mixed-technology printed-circuit boards.

ECSS 'Space Mechanisms Standard Requirements Specification' (draft).

Labruyère, G. & Urmston, P. (1995). *ESA Mechanisms Requirements*. Proc. 6th European Space Mechanisms and Tribology Symposium.

The test laboratory shall also fulfil the requirements specified in ISO 9001 and EN 29001.

For comparability reasons the material and test parameters shall be documented using a standardised form,[2] as shown in Fig. 21 of ESA STM-279 [B2].

Since this test is related to space tribology, the common requirements are based on ESTL (1995). *Tribometer User's Guide for Space Mechanism Applications*, ESTL/TM/139.

B.2.3 Abbreviations and definitions

See section B.7.

---

[1] At present, it is not the aim to investigate the 'static friction force', i.e. the force needed to start sliding.

[2] DIN 50 324 'pin-on-disc wear test' was rejected on 27 November 1997.

B.3 Preparatory conditions

B.3.1 Hazards/safety precautions

Readers are reminded that the following devices use hazardous voltages: ion getter pumps, piezo-translators and glow discharge devices.

B.3.2 Material specimens and equipment

B.3.2.1 Specimens

B.3.2.1.1 Identification of materials

Materials submitted for testing shall be identified by the customer using a form based on that shown in Fig. 21 of ESA STM-279 [B2]. If no material data are available (Y, E, ν, H), values shall be taken from the literature (E, ν), from tensile tests (Y) and from hardness tests (H). Calculation of the yield strength from Vickers hardness test shall be avoided.[3] If Y is used, this shall be accompanied by the index 'HV': $Y_{HV} = H_V / 2.6$.

B.3.2.1.2 Dimensions

The contact geometry refers to pin (spherical shape) on disc (flat). For standard testing (except for GD), the preferred dimensions are as follows (see section B.7.5, bottom sketch):

- *Pin:* diameter 6 mm, length 8 mm (consisting of a tip 4 mm in length and an external M3 thread 4 mm in length). The radius of curvature calculated by ARCS depends on the desired contact pressure, but ranges from 0.5 mm to 30 mm.

- *Disc:* diameter 21 mm, thickness 2–4 mm (for impact testing thicknesses up to 10 mm are possible).

If GD is applied, instead of a disc, a second pin with flat surface is needed (see section B.7.5 for illustrations):

- 2 pins: diameter 6 mm, length 8 mm (both including an internal M3 thread 4 mm in length), one with a flat surface and the other with a curved surface (the radius of curvature is calculated by ARCS depending on the desired contact pressure, but ranges from 0.5 mm to 30 mm).

B.3.2.1.3 Finish

The standard finish shall consist of grinding with paper to surface roughnesses of:

Disc: $R_a \leq 0.1 \pm 0.02$ µm
Pin: $R_a < 0.1$ µm (curvature)

[3] However, this is common practice in tribology, since the contact refers to a similar stress situation.

It is good practice even before cleaning to check the surface finish for scratches or adhering debris by visual inspection (using an optical microscope). The surface roughness must also be recorded. In the case of soft materials, and if no in situ glow discharge is applied, this may be done after the test, in order to prevent scratches resulting from the diamond stylus of the profilometer.

If not otherwise specified, the final grinding shall be done directly before the test, i.e. evacuation shall be started 30 minutes after completing the finish.

In addition, other finishes or coatings may be chosen in order to comply with definite applications. If the finish is not applied in-house, the samples must be sealed in suitable bags. The unsealing of protection bags, and the removal of samples, shall be done less than 30 minutes before commencement of the test.

B.3.2.2 Cleaning/handling

The cleaning procedure shall be similar to that applied during construction of the mechanism. If not otherwise specified, the following standard procedure will be followed after machining and directly before the test:

- ultrasonic bath in a suitable solvent for at least 10 min at ambient temperature
- ultrasonic bath in acetone for at least 1 min at ambient temperature

The cleanliness should be checked using a light microscope.

Suitable solvents include ethanol (99.5%), propanol (99%), deionised water at 40°C (drying necessary), trichloroethane and acetone (99%). For the standard solvent, trichloroethane is used.

Handling and storage

Before and after the test, until post-investigations, mechanical damage of the contacting surfaces should be avoided. Great care should also be taken not to recontaminate the surfaces between cleaning and the test. The samples should be handled only with lint-free gloves (for environmental conditions, see below).

B.3.2.3 Laboratory

Cleanliness
The working area shall be clean and free of dust. Air used for ventilation shall be filtered to prevent contamination of samples by moisture, oil or dust.

Environmental conditions
The room temperature shall be held constant during a test. The relative humidity shall be less than 50% RH, and the temperature within 22 ± 4°C. If a control is not possible, it is recommended that the two parameters are recorded with an accuracy of less than ±2°C and ±5% RH, respectively.

B.3.2.4 Equipment – special apparatus

B.3.2.4.1 Description of special apparatus

The facility shall simulate the closing and opening of a mechanism. After an optional impact, the contact is held closed with a defined load, within

which fretting may be applied but shall be stopped before unloading. At each separation the vertical force necessary to separate the pin and the disc, i.e. the adhesion force, shall be measured. This sequence (or cycle) shall be repeated several thousand times fully automated.

During adhesion tests the *vacuum system* shall be pumped by an ion getter pump to ensure vibration-free measurements and to avoid oil contamination (e.g. in the case of a diffusion pump). In addition, the chamber shall be fixed on a heavy ground plate to provide vibration damping. For static testing an air damping system is required.

Before the test, *in situ glow discharge (GD) cleaning* of the contact surfaces should be possible. Therefore, suitable gas inlet pipes and valves, low vacuum gauges, a high-voltage source and a voltmeter are necessary. A shutter that can be moved between pin and disc during the GD process shall be available; otherwise cross-contamination can occur. Both sample surfaces have to be taken as cathodes and the vacuum chamber and the shutter act as the anode. In addition, all parts connected to high voltage must be shielded in order to expose only the contact surfaces to the GD.

The *tribo-system* shall consist of a movable pin with a spherical tip and a fixed disc. The movement of the pin shall be smooth, in order to prevent breaking the adhesive junctions before separation. To ensure the required sensitivity, all forces should be measured directly in the vacuum chamber. The impact energy may be determined outside the vacuum chamber by measuring the impact velocity. Loading shall be possible either slowly, i.e. static, or by an impact with a defined energy.

To enable independent selection of the impact energy and the subsequent static load, no dead-weight-like loading system shall be used. A *preferred setup* consists of a loading mechanism using an electromagnet outside the vacuum chamber. The load is applied via a pushrod through a bellow to the pin. The pushrod itself is suspended frictionless by springs. A piezo force transducer may be used for the measurement of all forces under vacuum. At each separation the force necessary to separate the pin and the disc vertically, i.e. the adhesion force, must be measured.

To enable controlled *impacts*, a suitable electronic device is necessary to provide the electromagnet with defined energy pulses. For the determination of the impact energy, the mass of the pushrod including the force sensor – the pin is neglected – and the impact velocity must be known. The latter shall be measured by an external distance sensor and recorded using a storage oscilloscope.

If *fretting* is selected, it must be applied only during closed contact and stopped before unloading. The horizontal force needs to be controlled in order to reduce any lateral force, which commonly exists after stopping fretting. Otherwise junctions would be sheared off during unloading and at the separation itself no adhesion would be measured. The fretting movement may be introduced by a plate using a piezo transducer and verified by a displacement sensor. Here, the lateral and vertical forces (load, adhesion) must be measured, which may be achieved by a 3-axis force transducer (see Fig. B.1).

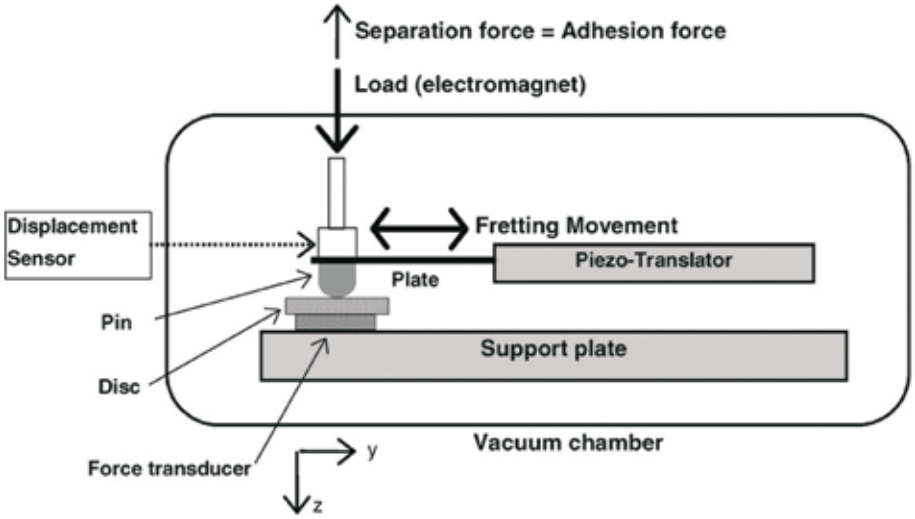

Fig. B.1. Functional sketch of a fretting device.

The *control and data acquisition software* must fulfil the requirements given below. The main requirement is to measure and acquire the adhesion force at each separation automatically.

B.3.2.4.2 Technical specifications

Requirements for equipment necessary to perform tests:

Vacuum, vibration damping	ion pumps, damping system
Vacuum (base pressure):	
static	$<1 \times 10^{-8}$ mbar
impact	$<5 \times 10^{-8}$ mbar
fretting	$<5 \times 10^{-7}$ mbar
'Frictionless' loading system	e.g. electromagnet (computer-controlled), pushrod suspended by springs
Applicable (static) loads:	
static, impact	1–100 N
fretting	1–40 N
Impact	
Energies:	0 (static) to 0.02 J (impact)
velocities (calculated from energies)	0 to 0.25 m/s
duration of contact and opening	selectable – seconds (typical) to hours
Fretting:	
oscillating frequency	2–200 Hz, triangle or sine wave.
sliding amplitude (max.)	10–60 µm
on/off control	(separation without fretting!)
control of amplitude	horizontal force has to be at zero before separation

Measurement and accuracies required:

Vacuum	UHV and low vacuum gauges
Impact velocity	±0.01 m/s, (energy: $\pm 2 \times 10^{-5}$ J)
Static load	±5% of load, ±1 N minimum
Adhesion force:	
static	±1 mN, drift <5 mN/min
impact	±10 mN
fretting	±50 mN
Fretting:	
sliding amplitude (max.)	±5 µm
horizontal force, accuracy	±0.05 N

Fully automated control by PC is at least required for:

- cycling
- separation sequence (adjusting the force sensitivity to the highest possible value)
- zeroing of horizontal force after fretting and before separation (a critical value is defined below)

Fully automated data acquisition by PC is at least required for:

- load
- vacuum
- adhesion force (value of each cycle, time resolution 25 ms)
- backup of separation sequence for maximum adhesion
- impact velocity
- impact force
- impact sequence (rebounds)
- fretting frequency, amplitude

Optional equipment for surface cleaning:

Glow-discharge cleaning	
Low vacuum control	~0.2 mbar, ±0.01 mbar,
High-voltage device	$U = -1100 \pm 100\ V_{DC}$, $I > 2$ mA (recommended: 2 mA/ cm^2)
HV measurement	$-1200 \pm 1\ V_{DC}$
Gas	Ar 5.0 with 5% H_2

Related equipment required for surface and material characterisation:

Profilometry	Mean surface roughness (R_a), max. peak-to-valley-distance (R_t)
SEM	Morphology and area of contact surfaces
EDX	Material transfer
Optical microscope	Visual inspection (cleanliness)
Hardness tester	Recommended for rapid calculation of contact parameters
Tensile test device	(Optional)

B.4 Test procedure

B.4.1 Selection of test parameters

Two criteria for the selection of test parameters are possible:

1. Standard test parameters (see below).
2. Test parameters according to the application (defined by the end-user).

For the purpose of setting up a database on adhesion/cold welding data, the standard parameters should also be included, e.g. at least by changing parameters during one test run. A flow chart is given in section B.4.3.

B.4.2 Test (contact) parameters

The main objective is to ensure the comparability of tests performed on all pairings of materials with different mechanical properties. The following parameters are chosen to be similar for all tests:

- Contact pressure relative to the elastic limit (EL),
- Impact energy (W) relative to the critical energy (W_Y).

Using Hertzian theory and the Tresca criterion, the critical static load related to the onset of yield, i.e. 100% EL, can be calculated (see section B.7.2):

$$P_Y = 21.17 \frac{R^2 Y^3}{E^{*2}} \quad \text{[N]} \qquad \text{(B1)}$$

The critical impact energy (W_Y), which is related to the onset of plastic yield at low-impact velocities, may be calculated according to the dynamic Hertzian theory (see section B.7.2):

$$W_Y = 53.4808 \frac{Y^5 R^3}{E^{*4}} \quad \text{[N]} \qquad \text{(B2)}$$

Static adhesion test

For the *contact pressure*, two values shall be used:

- Start test at the elastic limit according to Hertzian theory, i.e. 100% EL
- After reaching constant adhesion level, increase to 188% EL.

To achieve the required contact pressure, the radius of curvature (R) can be adjusted in the range from 0.5 mm to approximately 30 mm. This results in static loads within the ranges 5–10 N (100% EL) and 40–50 N (188% EL).

Impact adhesion test

For the *contact pressure,* three values shall be used:

- first 10 000 cycles at 40% EL
- next 5000 cycles at 60% EL
- next 5000 cycles at 100% EL.

As mentioned above, selecting a radius of curvature in the range 0.5–30 mm enables both static load conditions and the impact energy condition to be fulfilled. For standard testing, the *impact energy* shall be constant throughout the test:

- 40 * W_Y

For additional testing, the following impact energies are recommended:

- 200 or 4000 * W_Y

(*Note*: The parameters adopted are based on studies of the influence of impact parameters on adhesion [B3]; higher impact energies do not increase adhesion significantly.)

Fretting adhesion test

For the *contact pressure,* the following value shall be used:

- 50% EL

The fretting parameters themselves refer to a frequency of 200–220 Hz and an amplitude, the 'end-to-end-movement distance', of 50 µm. Fretting shall be applied for 10 s and then switched off.

Important: After fretting is stopped, a lateral force remains within the contact. Before unloading, this force must be reduced to a value <0.03 N. Otherwise, the welded contacts would be sheared off in a lateral direction during unloading, and at separation no (vertical) adhesion force would be measured.

The holding/resting durations for all test types are given in Table B.1. (The resting duration depends on the vacuum, i.e. the product of vacuum times resting shall be constant to achieve a defined recoverage of the surface during opening, i.e. a better vacuum allows longer resting.)

Table B.1. Overview of main test parameters

Contact type / Parameter	Static	Impact	Fretting	Static with GD
Vacuum required	<1 × 10^{-8} mbar	<5 × 10^{-8} mbar	<5 × 10^{-7} mbar	<5 × 10^{-8} mbar
Impact energy	–	40 W_Y (200, 4000 W_Y)	–	–
Fretting frequency Fretting amplitude			200 Hz 50 µm	
Contact pressure (% EL)	100, 188*	40, 60, 100	60	100
Static loads (N)	3–50 N	3–100 N	3–40 N	3–50 N
Holding time	30 s	10 s	10 s	1. Cycle: 900 s 30 s
Resting time	5 s	5–10 s	5–10 s	5 s

* Theoretical calculations.

Clarification of choice of parameters

The investigations on parameters reported in [B3] can reduce testing effort: for screening only, the use of one impact energy of 40 W_Y, i.e. the energy that first causes yield, is sufficient (higher impact energies did not increase adhesion significantly). It is combined with three different static loads (40%, 60% and 100% EL), which are subsequently applied within one test. An increase in contact pressure can induce irreversible changes in material properties (work hardening, yield). Hence, reducing the contact load from 'high' to 'low' would probably result in a too low contact area compared with a virgin surface (e.g. the contact area depends on the yield strength). This could also lead to a too low adhesion value.

On the other hand, for the contact properties, a previous lower load has no significant influence. Hence, testing can be done using increasing but not decreasing steps. To exclude the influence of running-in effects, a duration of 10 000 cycles for the first load, and 5000 cycles for each subsequent parameter, has been found to be sufficient.

B.4.3 Test process for general spacecraft applications

B.4.3.1 Flow chart

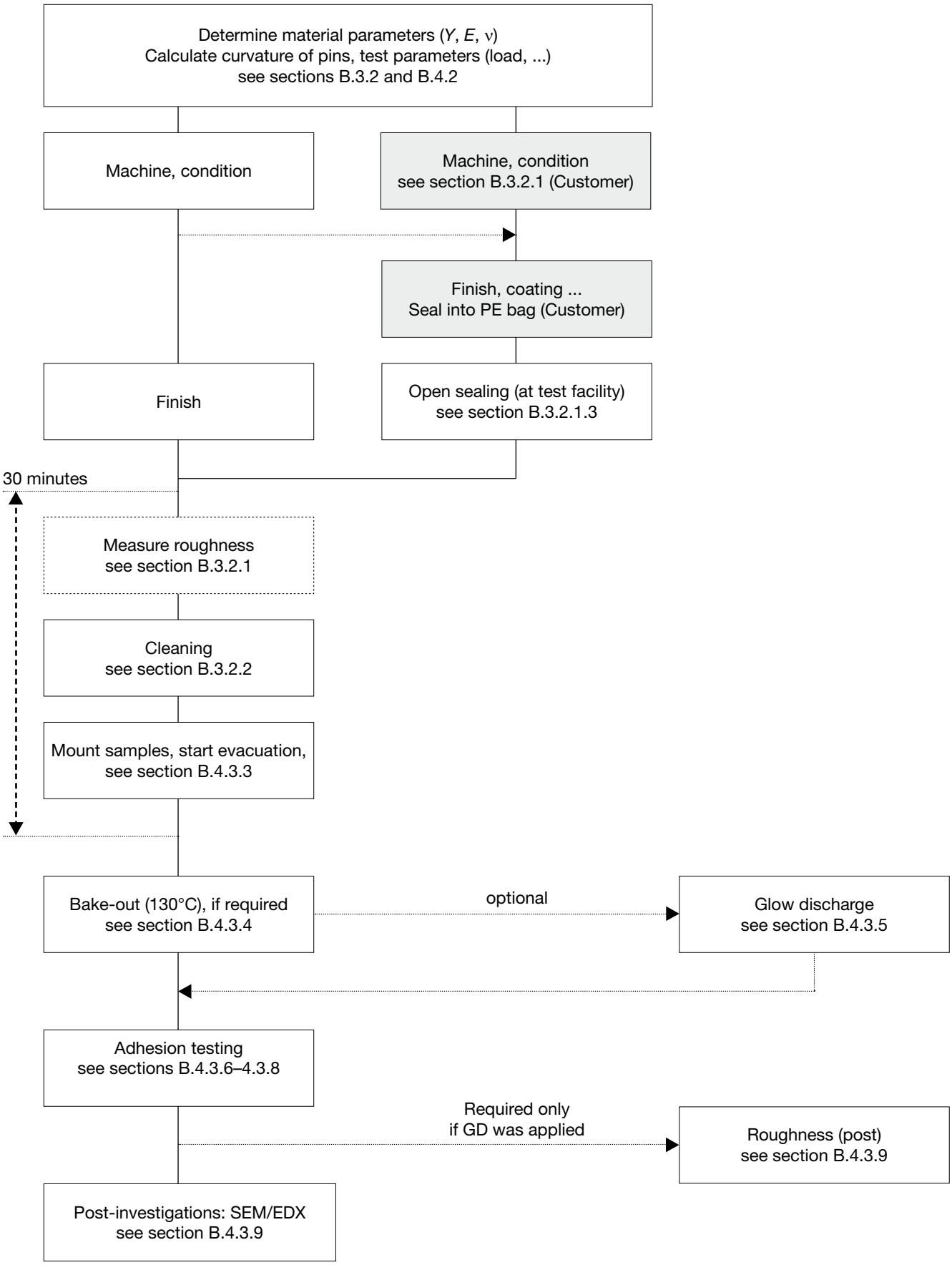

B.4.3.2 Sample preparation and pre-test investigations

For details of sample preparation, see section B.3.2, ‘Materials, specimen’, or the flow chart in section B.4.3.1: finish, roughness, cleaning procedure, cleanliness check, mounting of samples and start of evacuation. The duration of the period from completion of finish, or opening the sealing, to the start of evacuation shall be 30 minutes!

B.4.3.3 Sample mounting and functional checks

In the case of impact loading, the disc must be properly fixed to prevent it becoming loose. Care must be taken to avoid loading the contact by the air pressure during evacuation. In the case of force measurements by piezo transducers, the drift shall be low enough to ensure correct unloading control, e.g. <5 mN/min for a resolution of 20 mN/V. Ensure proper electrical insulation of the pin and the disc with respect to ground (vacuum chamber) if glow discharge is foreseen.

B.4.3.4 Evacuation and bake-out

The chamber is pumped down by a turbomolecular pump and baked out at 130°C (50 N-piezo), if it is necessary to achieve the required base pressure, i.e. for fretting tests it is not necessary. The ion getter pump may be turned on during bake-out. After cooling to room temperature, glow discharge cleaning may be included to achieve clean surfaces.

B.4.3.5 Glow discharge cleaning process

Before starting the DC glow discharge, the shutter must be moved between pin and disc to avoid cross-contamination. If surface analysis is not available to determine cleanliness, the voltage–pressure correlation must be observed. At constant pressure, voltage increases with reduction of impurity (oxide) layers. After voltage has become constant, the surface can be assumed to be clean. To improve the cleaning process, approximately 5% H_2 shall be added to the Ar.

The parameters for the GD cleaning process are:

Gas: Ar 5.0 with 5% H_2
Pressure: about 0.2 mbar, accuracy ±0.01 mbar
DC voltage: –1100 ± 50 V, accuracy ±1 V
Current: 2 mA/cm^2
Duration: 20 min total, but at least 10 min at constant voltage, i.e. $\Delta U < \pm 5$V
Resting time: 30 s between GD and first loading

Between the end of glow discharge and loading the contact a resting time of 30 s shall be maintained. The holding time of the first cycle shall be 15 min. Within this time the chamber is evacuated, pumping shall be taken over by ion getter pump to ensure that the test continues vibration-free. The changes in the surface structure and roughness properties must be determined if GD has been applied.

B.4.3.6 Static/impact cyclic adhesion test

In the case of static loading the distance between pin and disc in the opened state shall be as low as possible in order to avoid vibrations induced by the movement. Check the drift of the piezo to ensure it is low.

To achieve the desired impact energy the pin–disc distance and the impact velocity have to be adjusted. If the latter is measured, an oscilloscope may be used and the impact energy may be calculated using the mass of the pushrod:

$$W = (m\, v^2) / 2 \qquad [\,\mathrm{J}\,]$$

The parameters of the contact – load level, duration of contact, duration of open contact, loading/unloading speed – are controlled by computer. It is good practice to confirm the correct process control of the PC during the first 10 cycles, and to acquire the adhesion force every few thousand cycles.

B.4.3.7 Change of parameters

For economic reasons, and if only the destruction in the most severe case is of interest, the load, holding and resting duration, as well as the impact energy may be varied after a steady state has been achieved by the former set of parameters. Due to the probability of work hardening, only the load or the impact energy values should be increased (see section 4.2 and e.g. Table 1).

B.4.3.8 End of test

In all three types of test, the cycling may be stopped when

1. the steady state of the adhesion force is determined, or
2. the standard number of cycles is achieved, or
3. the desired lifetime, i.e. number of cycles, is achieved.

B.4.3.9 Post investigations

During unloading of the samples, the presence of debris shall be noted. Especially if GD cleaning has been applied, any changes in the surface structure and the surface roughness must be determined by SEM and a profilometer, respectively. At least the contact area and possible material transfer shall be detected (in the case of static loading and rough surfaces it may be impossible to detect the contact area, so the theoretical values may be taken).

B.5 Acceptance limits

According to the ECSS E-ST-33-01C (2009) ‘Space Mechanisms Standard Requirements Specification’, the designers of space applications must meet the following mechanical requirements:

- A Hertzian contact pressure less than 50% of the yield limit of the weaker material, and
- the actuator that separates the contact surfaces must provide three times the worst possible adhesion force under representative environmental conditions.

→ Hence, if the designer of the mechanism has specified the force of the separating actuator, the adhesion force must not exceed 30% of this force.

B.6 Quality assurance

B.6.1 Data

B.6.1.1 General

For practical reasons, a test protocol shall be written and should including all the data mentioned in this sub-section. If required, the Hertzian pressures may be given in an additional chart. This protocol may in future be replaced by a 'data sheet' containing the same data, but in a format that is more convenient for designers.

B.6.1.2 Material and surface data

Pin: Dimensions (radius of curvature), material (designation, composition, treatment, finish, Young's modulus, Poisson's ratio, hardness) and, if possible, the roughness (R_a = mean roughness, R_t = maximum peak-to-valley distance).

Disc: Dimensions (diameter, thickness), material (designation, composition, treatment, finish, Young's modulus, Poisson's ratio, hardness) and roughness (R_a, R_t).

B.6.1.3 Test parameters

Medium/environment: air, gas type, pressure.

Cleaning: before: US, in situ glow discharge cleaning.

Tribological parameters: geometry, impact (actual energy and critical value to initiate yield, peak force), static load(s) and corresponding Hertzian pressures, holding and resting time(s), cycles when parameters were changed (e.g. load, pressure, end of test), temperature, fretting frequency and amplitude.

B.6.1.4 Results

Adhesion force: at the beginning, the maximum for each set of parameters, the total maximum value.

Common descriptions: diameter of contact area (if detectable), changes in surface structures and material transfers of pin and disc, presence of debris.

Additional:

Diagram: adhesion force, mean and maximum of an interval of 100 cycles, as function of cycles.

B.6.2 Non-conformance

Any non-conformance – e.g. an interruption due to a power failure – must be documented.

B.6.3 Calibration

All measuring equipment, including the data acquisition, should be calibrated and any suspected or actual failures documented.

B.6.4 Traceability

To ensure the traceability of all specimens, each one is accompanied by a sample life sheet.

B.7 Abbreviations and definitions

B.7.1 Abbreviations – properties

US ultrasonic (bath)
GD glow discharge
HV high voltage
SEM scanning electron microscope
RH relative humidity
R_a mean roughness (arithmetic),
R_t maximum peak-to-valley distance

Contact parameters:
H_V Vickers hardness
Y yield strength
Y_{HV} yield strength calculated from the Vickers hardness
p_m mean contact pressure in the contact area
p_0 maximum contact pressure
P load (P_Y refers to load at the elastic limit)
R radius of curvature (spherical to flat contact; otherwise refer to e.g. ref. [B4])
E Young's modulus (of material 1: E_1)
ν Poisson's ratio (of material 1: ν_1)
E^* reduced Young's modulus (for formulas, see section B.7.2)
W impact energy (W_Y refers to the energy that first causes yield)
m mass (here of the pushrod)
v velocity

B.7.2 Hertz's theory of elastic contact

The following formulas are used to calculate the diameter of contact (a), the maximum contact pressure (p_0) and the mean contact pressure acting in a spherically shaped contact within the elastic regime (for the theory, see e.g. [B4], pp.93f):

$$\frac{1}{E*} = \frac{1-\nu_1^{\,2}}{E_1} + \frac{1-\nu_2^{\,2}}{E_2} \qquad [\text{Pa}]^{-1} \qquad \text{(B3)}$$

$$a = \left(\frac{3PR}{4E*}\right)^{1/3} \qquad [\text{m}] \qquad \text{(B4)}$$

$$p_0 = \frac{3}{2}p_m = \frac{3P}{2\pi a^2} = \left(\frac{6PE*^2}{\pi^3 R^2}\right)^{1/3} \qquad [\text{Pa}] \qquad \text{(B5)}$$

The elastic limit is related to the onset of yield (which occurs not at the surface but inside the softer material). Both the Tresca and von Mises criteria yield the same relation (see [B4], p.155):

$$p_0 = 1.60Y \qquad [\text{Pa}] \qquad \text{(B6)}$$

$$P_Y = \frac{\pi^3 R^2}{6E*^2}\left(p_0\right)_Y^3 \qquad [\text{N}] \qquad \text{(B7)}$$

Thus the load (P_Y) necessary to cause onset of yield follows:

$$P_Y = \frac{\pi^3 R^2}{6E*^2}\left(1.60Y\right)^3 = 21.17\frac{R^2Y^3}{E*^2} \qquad [\text{N}] \qquad \text{(B8)}$$

Using the yield criterion, Hertzian theory can also be used to calculate the (kinetic) energy (W_Y) necessary to cause yielding (see [B4], p.361):

$$W_Y = 53.4808\frac{Y^5R^3}{E*^4} \qquad [\text{J}] \qquad \text{(B9)}$$

For the definition of the impact velocity at ARCS, the mass of 0.48 kg is used:

$$v = \sqrt{\frac{2W}{m}} = 2.041\sqrt{W} \qquad [\text{m/s}] \qquad \text{(B10)}$$

B.7.3 Definitions – adhesion properties

Adhesion force: The force needed to separate two bodies in the vertical direction.

Adhesion coefficient: The adhesion force divided by the (static) load (i.e. the load applied after impact, not the impact force).

Static friction force: The force needed to start sliding, i.e. to shear off junctions in the contact plane, also referred to as stiction or sticking.

B.7.4 Definitions – quality assurance

Non-conformance: An apparent or proven condition of any item or documentation that does not conform to the specified requirements, or which could lead to the incorrect operation or performance of the item or mission. The term non-conformance is also used to refer to a failure, discrepancy, defect, anomaly, malfunction, deficiency, etc.

Traceability: The ability to trace the history, application, use and location of an item through the use of recorded identification numbers.

References to Annex B

[B1] Merstallinger, A., Semerad, E., Preissner, E. & Scholze, P. (1998). *Influence of Fretting on Cold Welding of Stainless Steel SS440C versus Ti-IMI 834 under Vacuum, Helium and Air*. ESTEC Contract no. 9198/89/NL/LC; Work Order no. 46, March 1997.

[B2] Merstallinger, A., Sales, M., Semerad, E. & Dunn, B.D. (2009). *Assessment of Cold Welding between Separable Contact Surfaces due to Impact and Fretting under Vacuum*. ESA STM-279, European Space Agency, Nordwijk, the Netherlands.

[B3] Merstallinger, A., Semerad, E. & Scholze, P. (1998). *Influence of Impact Parameters on Adhesion – Repeatability of Test Results*. ESTEC Contract no. 11760/95/NL/NB, Call-off Order no. 12, June.

[B4] Johnson, K.H. (1985). *Contact Mechanics*. Cambridge University Press.

B.7.5 Dimensions and forms of specimens

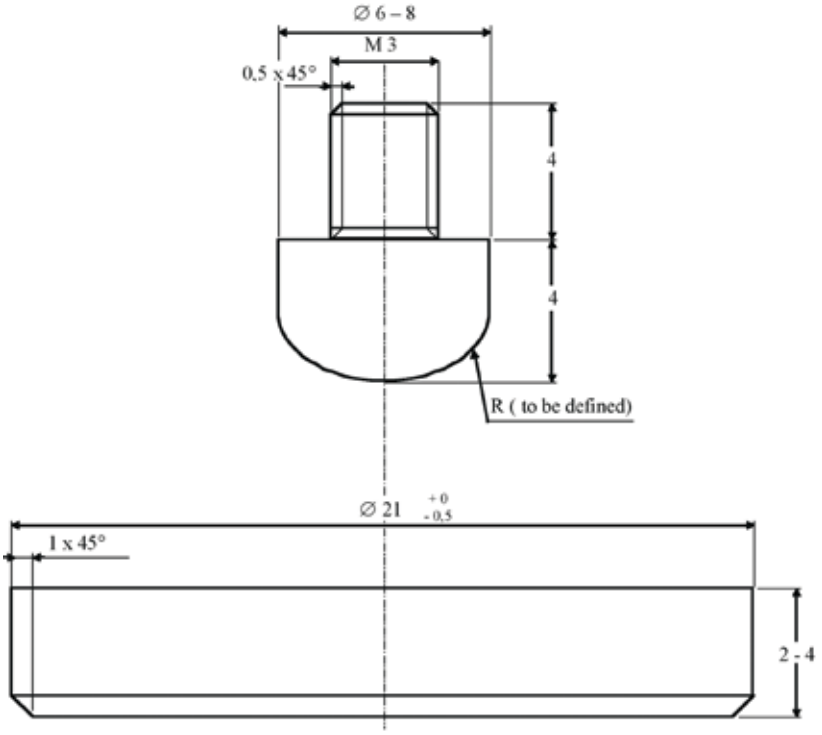

Specimen for static, impact, fretting tests

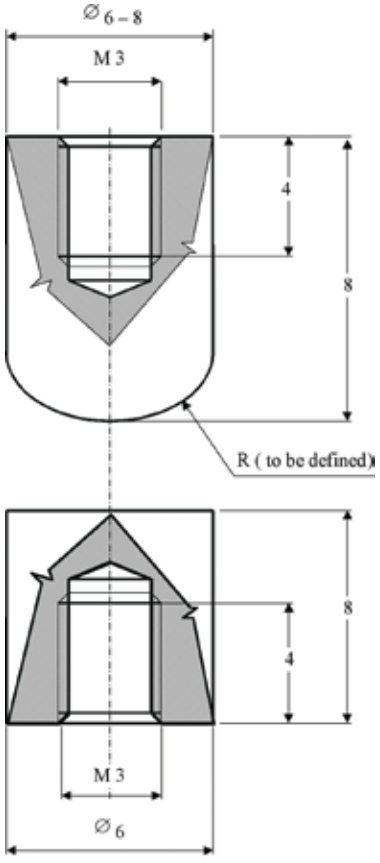

Specimens for GD-Test

Annex C: ‘Cold weld data’ database – summary tables

This annex shows summary tables that were printed out in July 2009. The actual data can be obtained from the AIT website:

http://service.arcs.ac.at/coldwelddata/

The tables are based on the classification discussed above. In the tables on the website, clicking on the symbol in the left column opens the data sheet for the test, with full details of materials, test parameters and results.

Cold Weld Data - Fretting

The summary table shows all data available for the pin-disc combinations in fretting. Look in lines for the discs and in rows for pins. Click on symbol to open detailed "Data Sheet"

The summary tables are based on following classification:

Symbol	Adhesion force [mN]		Comment to adhesion	Comment to Use
	lower limit	upper limit		
●	0	200	No or negligible adhesion, noise of test	Use recommended
◑	201	500	Small measureable adhesion	Security measures to be undertaken
◔	501	5000	Strong adhesion	Direct use not recommended
○	5001	higher	Severe adhesion	Direct use not recommended

Cold Weld Data

Home About ColdWelding **Table Fretting** Table Impact Contact Logout

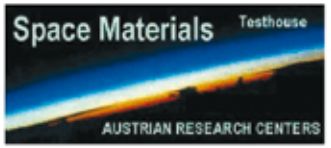

Home

Fretting

View Edit Outline

Cold Weld Data - Fretting

The summary table shows all data available for the pin-disc combinations in fretting. Look in lines for the discs and in rows for pins. Click on symbol to open detailed "Data Sheet". Test method is described in in ARCS-in-house-specification.

The summary tables are based on following classification:

Symbol	Adhesion force [mN]		Comment to adhesion	Comment to Use
	lower limit	upper limit		
●	0	200	No or negligible adhesion, noise of test	Use recommended
◑	201	500	Small measureable adhesion	Security measures to be undertaken
◔	501	5000	Strong adhesion	Direct use not recommended
○	5001	higher	Severe adhesion	Direct use not recommended

Disk	Pin	Material	Ag/MoS2	Al AA2219	Al AA7075	Al AA7075	Bronze LB9	Inconel 718	Steel SS 15-5 PH	Steel SS17-4	Steel SS17-7 PH	Steel SS17-7 PH	Steel AISI 52100	Steel AISI 316L	Steel AISI 440C	Ti Ti6Al4V	Ti IMI 318
	Coating	/	Keronite 2nd.40µ	/	Hard Anodised	/	/	/	/	/	TiC	/	/	/	/	/	
Material	Coating																
Ag10Cu	/		◔														
Al AA2219	Keronite2-40µ (AR)			◑									●●				
Al AA2219	Keronite2-40µ (AR)			◑									●●				
Al AA2219	Keronite2-40µ (TC)												●●				
Al AA2219	Keronite3-17µ (AR/TC)												●●				
Al AA2219	Keronite3-22µ +MoS2 (AR/TC)												●●				
Al AA2219	Keronite3-35µ (AR/TC)												●●				
Al AA2219	Keronite3-55µ +MoS2 (AR/TC)												●●				
Al AA6082	Keronite3-30µ (AR/TC)												●●				
Al AA7075	/				○												

AlAA7075	NiCr-plated					●											
AlAA7075	Hard Anodised								◑								
AlAA7075	Alodine				◔												
AlAA7075	Keronite3-40µ (AR/TC)												●●●				
AlAA7075	Keronite3-55µ +MoS2 (AR/TC)												●●				
Densimet D175	/									◔							
Inconel 718	/							○○									
Steel SS17-7 PH	/										○○						
Steel SS17-7 PH	MoS2										○○						
Steel SS17-7 PH	Nitrided						◔◔				○◔						
Steel SS17-7 PH	TiC										◔						
Steel AISI 52100	/										◔		◔				
Steel AISI 52100	DLC										◔						
Steel AISI316L	/													○○			
Steel AISI440C	/										◔◔◔				◔◔◑		
Steel AISI440C	MoS2										◑	◔					
Steel AISI440C	Braycote601														◑		
Ti - IMI834	/														○		
Ti-T6AlV	/														○○	◔	◔
Ti-T6AlV	MoS2															◔	
Ti-T6AlV	Dicronite DL5															◔	
Ti-T6AlV	Balinite A															◔	
Ti-T6AlV	Balinite B															◔	
Ti-T6AlV	Dicronite +															○	
Ti-T6AlV	Ni+PTFE															●	
Ti-T6AlV	CrN															◔	
Ti-T6AlV	TiB2															●	
Ti-T6AlV	Keronite 6µm															◔●	
Vespel SP3	/										●						

Cold Weld Data

Home About ColdWelding Table Fretting **Table Impact** Contact Logout

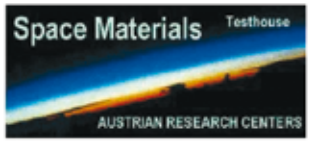

Home

Impact

View Edit Outline

Cold Weld Data - Impact

The summary table shows all data available for the pin-disc combinations in impact. Look in lines for the discs and in rows for pins. Click on symbol to open detailed "Data Sheet". Test method is described in ARCS in-home specification.

The summary tables are based on following classification:

Symbol	Adhesion force [mN]		Comment to adhesion	Comment to Use
	lower limit	upper limit		
●	0	200	No or negligible adhesion, noise offset	Use recommended
◑	201	500	Small measureable adhesion	Security measures to be undertaken
◔	501	5000	Strong adhesion	Direct use not recommended
○	5001	higher	Severe adhesion	Direct use not recommended

Disk	Pin	Material	Ag/MoS2	Al AA2219	Al AA7075	Al AA7075	Al AA7075	Bronze LB9	Inconel 718	Steel SS 15-5 PH	Steel SS17-4	Steel SS17-7 PH	Steel SS17-7 PH	Steel SS17-7 PH	Steel AISI 52100	Steel AISI 316L	Steel AISI 440C	Ti Ti6Al4V	Ti IMI 318
		Coating	/	Keronite 2nd 40µ	/	Hard Anodised	Alodine	/	/	/	/	/	MoS2	TiC	/	/	/	/	/
Material	Coating																		
Ag10Cu	/		●●																
Al AA2219	Keronite2-40µ (AR)			●											●●				
Al AA2219	Keronite2-40µ (TC)																		
Al AA2219	Keronite3-17µ (AR/TC)																		
Al AA2219	Keronite3-22µ +MoS2 (AR/TC)																		
Al AA2219	Keronite3-35µ (AR/TC)																		
Al AA2219	Keronite3-55µ +MoS2 (AR/TC)																		
Al AA6082	Keronite3-30µ (AR/TC)																		
Al AA7075	/				◔◔														
Al AA7075	NiCr-plated					●													
Al AA7075	Hard Anodised						●			●									
Al AA7075	Alodine				◑														

Al AA7075	Keronite3-40µ (AR/TC)																		
Al AA7075	Keronite3-55µ +MoS2 (AR/TC)																		
Densimet D175	/																		
Inconel 718	/								◔										
Steel SS17-7 PH	/											◔◔◔◔◔							
Steel SS17-7 PH	MoS2											●●	●						
Steel SS17-7 PH	Nitrided							●				◔							
Steel SS17-7 PH	TiC											◑●●		◑					
Steel AISI 52100	/											◑			●				
Steel AISI 52100	DLC											●							
Steel AISI316L	/															◑			
Steel AISI440C	/											●					◔●		
Steel AISI440C	MoS2																		
Steel AISI440C	Braycote601																●		
Ti - IMI 834	/																		
Ti-Ti6Al4V	/																◑◑	◔●●	
Ti-Ti6Al4V	MoS2																	◔	
Ti-Ti6Al4V	Dicronite DL5																	◑	
Ti-Ti6Al4V	Balinite A																	●	
Ti-Ti6Al4V	Balinite B																	●	
Ti-Ti6Al4V	Dicronite +																	●	
Ti-Ti6Al4V	Ni+PTFE																	●	
Ti-Ti6Al4V	CrN																		
Ti-Ti6Al4V	TiB2																		
Ti-Ti6Al4V	Keronite 6µm																	●	
Vespel SP3	/				●							●							

An ESA Communications Production